Virology 424 (2012) 115–128

Contents lists available at SciVerse ScienceDirect

Virology

journal homepage: www.elsevier.com/locate/yviro

The transcriptome of the adenovirus infected cell

Hongxing Zhao [a,*], Martin Dahlö [b], Anders Isaksson [b], Ann-Christine Syvänen [c], Ulf Pettersson [a]

[a] Department of Immunology, Genetics and Pathology, Rudbeck Laboratory, Uppsala University, 751 85 Uppsala, Sweden
[b] Department of Medical Sciences, Cancer Pharmacology and Informatics, Uppsala University, 751 85 Uppsala, Sweden
[c] Department of Medical Sciences, Molecular Medicine, Uppsala University, 751 85 Uppsala, Sweden

ARTICLE INFO

Article history:
Received 7 October 2011
Accepted 8 December 2011
Available online 10 January 2012

Keywords:
Adenovirus type 2
cDNA sequencing
Deregulation of host cell gene expression
Virus and host cell interaction
IMR-90

ABSTRACT

Alternations of cellular gene expression following an adenovirus type 2 infection of human primary cells were studied by using superior sensitive cDNA sequencing. In total, 3791 cellular genes were identified as differentially expressed more than 2-fold. Genes involved in DNA replication, RNA transcription and cell cycle regulation were very abundant among the up-regulated genes. On the other hand, genes involved in various signaling pathways including TGF-β, Rho, G-protein, Map kinase, STAT and NF-κB stood out among the down-regulated genes. Binding sites for E2F, ATF/CREB and AP2 were prevalent in the up-regulated genes, whereas binding sites for SRF and NF-κB were dominant among the down-regulated genes. It is evident that the adenovirus has gained a control of the host cell cycle, growth, immune response and apoptosis at 24 h after infection. However, efforts from host cell to block the cell cycle progression and activate an antiviral response were also observed.

Introduction

By convention, the human adenovirus replication cycle is divided into two phases, an early and a late phase, which are separated by the onset of viral DNA replication. Based on temporal changes of the gene expression pattern as revealed by DNA microarray analysis (Zhao et al., 2007), adenovirus type 2 (Ad2) infection in human primary lung fibroblasts can be divided into four periods. The first period is from 0 to 12 h after infection before or shortly after adenoviral gene expression has commenced. During this time, changes in cellular gene expression are likely to be triggered by the virus entry process, such as attachment of virus to cell surface receptors, and its intracellular transport along microtubules. Toll-like receptors might also be involved in these processes and MyD88 seems to play a central role (Hartman et al., 2007). Most of the deregulated genes have functions linked to inhibition of cell growth (Granberg et al., 2006; Zhao et al., 2007). Therefore, growth suppression is most likely the first response of the host cell to the incoming virus. The second period covers the time from 12 to 24 h after infection and follows activation of the immediate early E1A gene. During this period, there is an increase in the number of differentially expressed cellular genes. About 50% of these genes are involved in cell cycle regulation, cell proliferation and antiviral response. The third period extends from 24 to 42 h after infection. By this time, the virus has gained control of the cellular metabolic machinery, resulting in an efficient replication of the viral genome. Additional changes in cellular gene expression are modest during this phase. During the fourth and last period, when the cytopathic effect becomes apparent, the number of down-regulated genes increases dramatically including many genes involved in intra- and extracellular structure.

The most intensive battle between the adenovirus and its host takes place during the second period after adenovirus genes expression has started. The major functions of the early gene products are to force the host cell to enter the S phase in order to provide optimal conditions for viral DNA replication and to suppress the host antiviral response. Adenoviruses encode several regulatory proteins within the early regions E1A, E1B, E3, and E4. The immediate-early E1A gene encodes two regulators of viral and cellular gene expression, the E1A-243R and E1A-289R proteins. The E1A proteins act as promiscuous transcriptional activators or repressors of cellular genes (Arany et al., 1995; Bagchi et al., 1990; Bannister and Kouzarides, 1995; Deleu et al., 2001; Flint and Shenk, 1997; Fuchs et al., 2001; Wu et al., 1987). E1A proteins are essential for promoting the host cell to enter the S phase. This is achieved by the binding of the E1A proteins to members of the retinoblastoma tumor suppressor (pRB) family, thereby releasing the E2F transcription factors, which are activators of genes required in the S-phase (Bayley and Mymryk, 1994; Cobrinik, 1996). By microarray analyses it was shown that a significant fraction of the up-regulated genes during the early phase of infection are E2F targets (Miller et al., 2007; Zhao et al., 2003, 2007).

E1A-induced cell proliferation also involves interaction with chromatin-modifying and transcriptional coactivator complexes. The interaction between E1A and the coactivators p300 and the cyclic AMP response element-binding protein (CBP) probably disrupts the

* Corresponding author. Fax: +46 18 471 4808.
E-mail address: hongxing.zhao@igp.uu.se (H. Zhao).

0042-6822/$ – see front matter © 2011 Elsevier Inc. All rights reserved.
doi:10.1016/j.virol.2011.12.006

histone acetyltransferase activity of p300/CBP and the associated factor PCAF, leading to decreased transcription from a variety of genes, including those involved in growth arrest, cell differentiation, and immune evasion (Debbas and White, 1993; Lowe and Ruley, 1993). In addition, E1A interacts with TRRAP, which is a component of three distinct histone acetyltransferase complexes. Thus, E1A has the capacity to interact with multiple histone acetyltransferase complexes and recruit these to viral or selected cellular promoters. The interaction of E1A with p400/TRRAP (Deleu et al., 2001; Fuchs et al., 2001) and the co-repressor C-terminal Binding Protein (CtBP) (Chinnadurai, 2004; Johansson et al., 2005), provides additional possibilities for E1A to deregulate cellular transcription. It has, moreover, been shown by Ferrari et al. (2008) that cells are reprogrammed epigenetically as a result of specific E1A interactions at different times after infection. Therefore, the ability of E1A to target different cellular transcriptional regulators creates a variety of possibilities to deregulate the cell growth controlling activities of the host. Finally, E1A can block the growth inhibition mediated by TGF-β pathway (Coussens et al., 1994a; Datto et al., 1997a; de Groot et al., 1995).

A possible negative consequence of the S-phase induction is that the binding of E1A to pRb and p300/CBP promotes p53 accumulation, which leads to the induction of p53-dependent apoptosis (Debbas and White, 1993; Lowe and Ruley, 1993). E1A can also sensitize infected cells to TNFα- and TRAIL-induced apoptosis (Chen et al., 1987; Duerksen-Hughes et al., 1989; Routes and Cook, 1990). Adenoviruses have, however, numerous mechanisms, which can block apoptosis. Two E1B proteins, the E1B-55K and E1B-19K, play a major role in the counteraction of the pro-apoptotic program. E1B-55K binds to p53 (Yew et al., 1994), which promotes degradation of p53 through an E4orf6-E3 ubiquitin ligase complex (Punga and Akusjarvi, 2000; Querido et al., 2001). In spite of these compelling findings it was recently demonstrated that the p53 dependent genes are still repressed after infection with a mutant that is unable to express E1B-55K (Miller et al., 2009). The E1B-19K protein is a viral Bcl-2 homologue that acts as a broad inhibitor of mitochondria-dependent apoptosis (Farrow et al., 1995; Han et al., 1996). It can moreover interfere directly with the activity of p53 when translocated to the mitochondria (Lomonosova et al., 2005). In addition, E1A also counteracts its own induction of p53 through sequestering of p300/CBP (Somasundaram and El-Deiry, 1997). Furthermore, proteins encoded by the E3 transcription unit also inhibit apoptosis. E3-gp19K prevents exposure of viral peptides on the cell surface by inhibiting the transport of class I major histocompatibility complex from the ER to the plasma membrane, as well as inhibiting the loading of peptide by tapasin (Bennett et al., 1999; Burgert et al., 1987; Wold et al., 1999). The E3-10.4K and 14.5K (RIDα/β) complex inhibits tumor necrosis factor alpha (TNFα) and Fas ligand-induced cell death through internalization of the death domain containing receptors, which are subsequently degraded in the lysosome. In addition, the E3-10.4K/14.5K complex can block the activation of NF-κB by preventing NF-κB from entering the nucleus, as well as by inhibiting the activity of the kinase complex IKK (Friedman and Horwitz, 2002). Although E1A is responsible for the increased TNFα sensitivity (Ames et al., 1990), E1A also balances this induction by interfering with the transcriptional activity of NF-κB (Cook et al., 2002) by targeting the p300/CBP co-activators, and by inhibiting NF-κB acetylation (Jennings-Gee et al., 2006) and IKK inhibition (Shao et al., 1999).

Following the accumulation of E2 gene products, adenovirus DNA replication starts and the viral transcription switches from the early to the late mode. Through a shift in splice site selection, E1A expression is changed from an early preference for the 289R transcriptional activator to producing the shorter E1A-243R protein during the late phase of the infection (Chow et al., 1979). The E1A-243R protein mainly functions as a transcriptional repressor through its capacity to bind p300/CBP (Jones, 1995). The L4-100 kDa protein expressed from the major late transcription unit also regulates viral gene expression and shuts off translation of cellular mRNAs (Cuesta et al., 2000; Farley et al., 2004; Hayes et al., 1990). A dramatic down-regulation of cellular gene expression was noticed at very late stage of infection (Zhao et al., 2007). Most of these genes are involved in maintaining intra- and extracellular structure.

We and others have previously studied the temporal host cell transcription profiles in adenovirus-infected human fibroblasts using microarray analysis (Granberg et al., 2006; Miller et al., 2007; Zhao et al., 2003, 2007). More than two thousand unique cellular genes were identified as differentially expressed in infected cells as compared to uninfected cells. In our previous studies, nine time points from 2 up to 48 h after infection were examined. Several important cellular functions were deregulated during the infectious cycle. The microarray studies represent a starting point in the unraveling of the dynamics of the transcriptome during a virus infection. With the development of high-throughput sequencing technologies, the transcriptome can be explored on a genome-wide scale at single base pair resolution. This methodology has clear advantages when compared to microarray analysis. Firstly, the measurements of transcription levels are much more precise. Secondly, the entire cellular genome can be interrogated, including non-coding genes and intergenic regions. Here, we describe a study of host cell transcription profiles by sequencing of the total RNA pool in adenovirus infected cells.

Results and discussion

RNA expression profiles in adenovirus infected human primary lung fibroblasts

Here, we have applied cDNA sequencing to study differences in the cell transcription profiles at different times after adenovirus infection. The design of the experiments was similar to that used in our previous microarray study (Zhao et al., 2007). Human primary lung fibroblasts (IMR-90) were synchronized prior to infection by contact growth inhibition and infection was performed at a multiplicity of 100 FFU per cell. Cells were harvested at 12 (Ad-12 hpi) and 24 hpi (Ad-24 hpi), as well as after mock infection and total RNA was extracted to be used for the cDNA library preparation. Previous results show that 12 and 24 hpi represent critical time points in the adenovirus infectious cycle (Zhao et al., 2007). At 12 hpi, expression of cyclin E1 is detected, demonstrating that the infected cells had progressed into the late G1 phase of the cell cycle. At 24 hpi, adenovirus DNA replication has started indicating that the late phase of the infection has begun. Thus, examination of cellular gene expression at 12 hpi and 24 hpi should reflect two critical stages of the infectious cycle.

Three cDNA libraries, mock, Ad2-12 hpi and Ad2-24 hpi, were sequenced and yielded 50–54 million 76 bp long sequence reads per sample, as shown in Table 1. More than half of the reads from each sample (59.6–65%) could be aligned to the human and adenovirus genomes. The fraction of reads that aligned to the human reference genome decreased following adenovirus infection, from 31.7 million reads in the mock infected sample to 19 million reads at 24 hpi. Correspondingly, the reads aligned to the adenovirus genome increased dramatically, from 401 to 15.9 million reads. The 401 reads that were aligned to the adenovirus genome in the mock sample represented

Table 1
Summary of sequencing reads and alignment to the human and adenovirus genome.

	Mock	Ad2-12 hpi	Ad2-24 hpi
Total sequencing reads	53,146,621	50,045,456	54,355,211
Alignment to both human and Ad genome	31,696,418 (59.6%)	30,907,561 (61.8%)	35,346,824 (65.0%)
Alignment to human genome	31,696,017 (100.0%)	29,549,310 (95.6%)	19,424,249 (55.0%)
Alignment to Ad genome	401 (0.0%)	1,358,215 (4.4%)	15,922,575 (45.0%)

the background noise. Out of 35 million aligned reads at 24 hpi, 45% matched the adenovirus genome, indicating a very efficient infection.

Expression of adenovirus genes occurred in a stepwise pattern. At 12 hpi, only the early genes, E1A, E1B, E3 and E4 were expressed (data not shown) and expression of E1A and E1B was lower as compared to the expression of E2A, E3 and E4. The complete absence of expression from the major late promoter was conspicuous. At 24 hpi, in contrast, the late viral genes were expressed at a very high level, indicating that the infection had efficiently proceeded into the late phase. Huge amounts of sequence reads covering exonic, intronic and intergenic regions were obtained in this study. However, in the present study we focused on the analysis of cellular exonic sequences.

Identification of 3791 cellular genes that were differentially expressed during the adenovirus infection

Using a 2-fold cut off level, 3791 cellular genes were found to be differentially expressed at 12 and 24 hpi. Among them, 1267 and 3683 cellular genes were identified at 12 and 24 hpi, respectively. Most of the differentially expressed genes identified at 12 hpi were sustained at 24 hpi, but with more dramatic changes. Only 108 genes were exclusively deregulated at 12 hpi. The 3791 differentially expressed genes were functionally annotated based on the DAVID (the Database for Annotation, Visualization and Integrated Discovery) bioinformatics resource. Genes in the output list were classified into gene groups, which were defined as functional categories. The gene members in each category shared common biological characteristics. As shown in Table 2A, cellular genes involved in DNA replication obtained the highest score value (=P-value of 10^{-21}). Cell cycle genes received the second highest score followed by genes participating in many cellular biosynthetic processes. Genes involved in regulation of cell growth followed next. Genes implicated in wound healing and intracellular structure also received high scores.

In order to compare genes that were deregulated at different time points, data obtained with the different cDNA libraries were analyzed separately and the results were shown in Table 2B and C. Although the number of differentially expressed genes increased dramatically from 12 hpi to 24 hpi, and more cellular functional pathways were affected at 24 hpi, many key targets were similar. Cellular genes involved in DNA replication and the regulation of biosynthetic processes were the most significantly regulated genes at both time points. Genes involved in the cell cycle and cell growth became more prominent at 24 hpi. A striking difference was that genes involved in angiogenesis/wound healing, apoptosis and cytoskeleton organization became significant at the later time point.

Table 2
DAVID functional annotation of 3791 differentially expressed genes identified from both Ad-12 hpi and Ad-24 hpi (A), differentially expressed genes identified at Ad-12 hpi (B) and at Ad-24 hpi (C).

Category	Functional annotation	Enrichment score
A		
1	DNA replication	21.4
2	Cell cycle	14.1
3	Regulation of biosynthetic process	8.5
4	Regulation of cell growth	6.0
5	Spindle/microtubule organization	5.7
6	Angiogenesis/wound healing	5.4
7	Regulation of cell proliferation	4.9
8	Organ development	4.5
9	Regulation of cell differentiation	4.3
B		
1	DNA replication	10.9
2	Regulation of biosynthetic process	6.4
3	Organ development	6.0
4	Regulation of cell proliferation	4.4
5	Cell cycle	3.6
C		
1	DNA replication	23.6
2	Cell cycle	14.5
3	Regulation of biosysnthetic process	7.2
4	Regulation of cell growth	6.8
5	Regulation of cell proliferation	5.0
6	Spindle/microtubule cytoskeleton organization	4.8
7	Angiogenesis/wound healing	3.9
8	Regulation of cell differentiation/developmental	3.8
9	Cytoskeleton organization	3.8
10	Regulation of apoptosis	3.7
11	Chromosome organization/modification	3.5

Clustering of differentially expressed genes and functional annotation of the clusters

Based on their expression patterns, the 3791 differentially expressed genes were broadly grouped into 6 clusters using Genesis (Fig. 1). Cluster 1 contained 13 genes, which were down-regulated only at 12 hpi and then returned to base line at 24 hpi. In contrast, genes in cluster 2 were up-regulated only at 12 hpi. More than half of the deregulated genes (1955 genes) were up-regulated and included into clusters 3 and 4. Genes in cluster 3 were up-regulated already at 12 hpi and remained up-regulated at 24 hpi, whereas up-regulation of genes in cluster 4 was seen first at 24 hpi. Nearly half of the differentially expressed genes were in cluster 4. Cluster 5 contained 1056 genes and their expression had decreased at 12 hpi and the deregulation was maintained at 24 hpi. Genes in cluster 6 were down-regulated at 24 hpi but not at 12 hpi. Among the deregulated genes, 71% were down-regulated at 12 hpi but the number was decreased to 35% at 24 hpi. More genes (65%) were activated at 24 hpi. Apparently, there was a switch from repression to activation of cellular gene expression. This seems rational since the virus needs to suppress the host antivirus response early after infection whereas late after infection genes involved in DNA and protein synthesis need to be activated for efficient virus production.

The functional annotations of genes in the 6 clusters were based on DAVID analysis as summarized in Table 3. Unfortunately, the genes in clusters 1 and 2 could not be functionally annotated because of their small number. However, by searching for functions, mostly using the Stanford data base SOURCE (http://smd.stanford.edu/cgi-bin/source/sourceSearch), Genecards (http://www.genecards.org) and PubMed (http://www.ncbi.nlm.nih.gov/pubmed), it became apparent that these two clusters contained genes with interesting functions. Cluster 1, for instance, included CDC20 and UBE2C, which were directly involved in cyclin ubiquitination and degradation, and HJURP, CSRP2 and EGR2 implicated in control of cell growth. Cluster 2 included a diverse set of genes involved in various biosynthesis processes. In addition, a broad range of genes involved in cellular signaling such as G-protein signaling, Wnt and Notch signaling were also transiently activated. These genes probably represented the first wave of deregulation of host cell gene expression.

Clusters 3 and 4 contained up-regulated genes, first detected at 12 and 24 hpi, respectively. Only two cellular functions were found to be significant in cluster 3, both related to DNA replication and nucleic acid biosynthesis. Although genes involved in cell cycle regulation did not stand out as significant, there were several key players in the G1/S progression in this cluster, such as Cyclin E, Cyclin F, CDC 7 and E2F6. Cluster 4, which was the largest cluster, included genes involved in the biosynthesis of DNA, RNA and protein, as well as the progression of the G1/S phase of the cell cycle. Examples of genes involved in DNA replication were DNA polymerases (POLA1, POLD1, POLD3, POLE, POLE2), all the minichromosome maintenance complex components (MCM2, MCM3, MCM4, MCM5, MCM6, MCM7, MCM8,

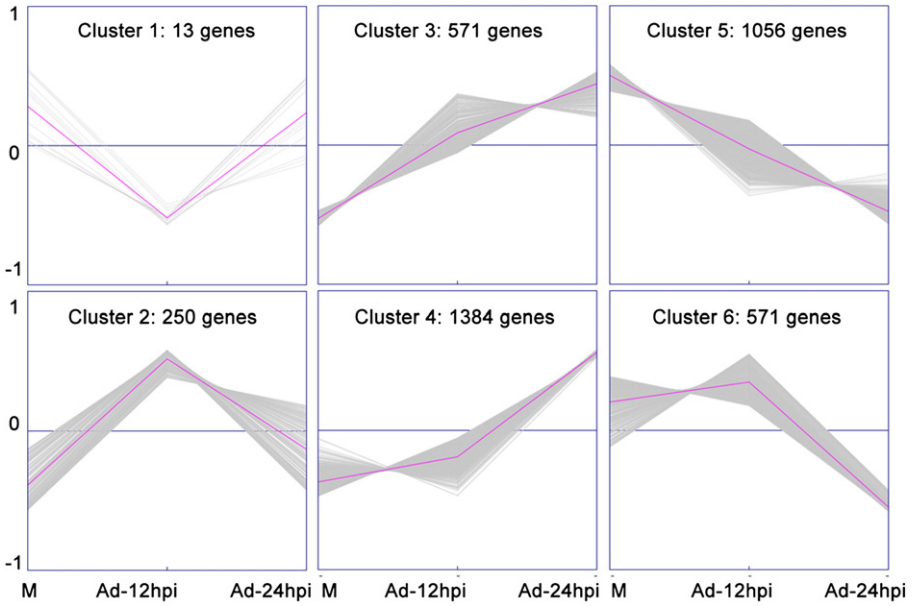

Fig. 1. The clusters of differentially expressed genes that were generated by Genesis. Each gene was normalized around zero with the "Normalize genes" function in Genesis and then k-means clustered. The purple line was the average expression pattern.

and MCM9), as well as replication factors (RFC2, RFC4 and RFC5). Genes implicated in cell cycle regulation included cyclins (CCNA2 and CCNB2), cyclin-dependent kinases (CDK1, CDK2, CDK4, CDK11B), and the cyclin-dependent kinase inhibitors (CDKN2A and CDKN2C) as well as CDC6, CDC23, CDC25A, CDCA2, CDCB29. The important transcription factors E2F1, E2F6 and E2F7 were also in this cluster.

Clusters 5 and 6 included down-regulated genes detected from 12 and 24 hpi, respectively. DAVID annotation analysis showed that genes in cluster 6 involved two cellular functions, namely vesicle trafficking and cytoskeletal components with relative low enrichment scores. However, the repression of genes involved in protein transport was broad and highlighted by genes in Rab subfamily (Rab14, Rab3A, Rab40C, Rab5B and Rab6C), involved in intracellular vesicle formation, trafficking and membrane fusion, and the Rho subfamily (such as RhoB, RhoT1) involved in regulation of cytoskeleton, as well as Rho related genes (ARHGEF1, and ARHGAP22). In addition, a group of genes involved in vesicle trafficking, such as the Sec23/Sec24 family (Sec24A, C and D, Sec23A) and Sec31 family (Sec 23A), as well as syntaxins (STX2 and STX7), synapotagmin 1 (SYT1), synaptophilin (SNPH and Rad21L1) and SNAP23, was also present in cluster 6. Furthermore, a large number of genes in the solute carrier family, such as SLC4A4, SLC5A3, SLC17A5, SLC25A30, SLC25A43, SLC26A1, SLC26A11, SLC30A1, and SLC35F5, were also included in the protein transport category. In contrast, genes involved in cellular structure were restricted, comprising collagen genes (COL1A1, COL5A1, COL6A3, COL8A1, COL12A1 and COL13A1), and a few genes encoding microtubule-associated proteins (MACF1, MAP1B and MAP2). Finally, a group of important genes implicated in TGF-β signaling (LTBP2, SMURF1, TGFBR2, BMPR2 and SMAD7) was present in cluster 6. The low enrichment score of cluster 6 suggested that the deregulation of genes involved in vesicle trafficking/protein transport and cellular structure was still limited at 24 hpi. This is consistent with our previous microarray study showing that down-regulation of the cytoskeleton and protein transport occurred at a very late stage of the infection, after 42 h (Zhao et al., 2007).

Table 3
DAVID functional annotation of genes in clusters 3, 4, 5 and 6.

Cluster	Category	Functional annotation	Enrichment score
3	1	Regulation of nucleic acid biosynthetic process	5.9
	2	DNA replication	3.1
4	1	DNA replication	31.7
	2	Cell cycle	30.9
	3	RNA processing	11.1
	4	Chromatid segregation/chromosome condensation	7.3
	5	Cellular macromolecular complex subunit organization	4.5
	6	Spindle/microtubule organization	4.3
	7	Nucleic acid biosynthetic process	3.6
	8	Telomere organization/maintenance	3.4
	9	Amino acid biosynthetic/metabolic process	3.2
5	1	Regulation of signal transduction	14.6
	2	Negative regulation of biological/metabolic process	10.9
	3	Cytoskeleton organization	9.3
	4	Angiogenesis/wound healing	8.7
	5	Tissue/organ development	7.8
	6	Regulation of apoptosis	7.2
	7	Regulation of cell proliferation	7.2
	8	Regulation of cell development/differentiation	7.1
	9	Regulation of cell growth/size	6.3
	10	Regulation of cell motion/migration	5.9
6	1	Vesicle trafficking/protein transport	3.4
	2	Cytoskeletal components/tissue morphogenesis	3.3

Cluster 5 contained a large set of genes, involved in several cellular functions and pathways (see Table 3). Genes implicated in cell signaling pathways were the most significantly suppressed gene group (category 1). In addition to TGF-β and NF-κB signaling pathways, genes involved in G-protein, Map kinase, as well as in FADD and FAS-mediated apoptosis pathway were also found to be down-regulated. When resubmitted to DAVID gene annotation analysis, genes included in category 1 could be further divided into positive and negative regulation of signaling pathways (data not shown here). Genes involved in TGF-β pathway were the most significant in the negative group, whereas genes involved in apoptosis were the most prominent in the positive group.

Genes in category 2 included genes involved in negative regulation of biological and metabolic processes, covering a very broad range of functions, such as growth, signaling, and apoptosis, which partially overlap with functions in the first annotation cluster. In contrast, genes in category 3 were more focused on cellular structure. Nearly half of the genes encode actin (ACTA1, ACTC1) and actin-

binding proteins, which were involved in actin nucleation and polymerization such as ARPC4, ARPC5, CNN1, CNN2, CNN3, FMN2, FMNL1, TMSB4X, TMSB4XP1, TMSB4XP2, TMSL3 and VASP. Category 4 included genes mainly involved in angiogenesis, including growth factors (FGF1, FGF2 CTGF, VEGFC TGFB and ANGPL4), receptors (FLT1, TGFBR1 and TNFRSF12A), and extracellular matrix and remodeling enzymes (MMP19, PLAT, PLAU, THBS1, CD9, CDH2 and RECK), as well as the angiogenic inducer CYR61. Down-regulation of these genes might suppress wound healing during the infection. In addition, several stress-induced genes, such as TXNRD1, HIF1A, ERCC2, and wound healing protein TPM1 were down-regulated.

Consensus binding sites for transcription factors in the promoter regions of differentially expressed genes

To investigate the mechanism by which the deregulation of cellular gene expression was accomplished, genes in the 6 clusters were scanned for the presence of consensus transcription factor binding sites using Transfind (Kielbasa et al., 2010), a software tool that predicts the affinity of a transcription factors to the promoter regions (−300 to +100). The gene list of each cluster was submitted as a positive set. The enrichment of transcription factor binding sites was measured relative to a gene set comprising all of the detected genes with more than two reads. The transcription factor matrix was defined as significant if the corresponding false discovery rate (FDR) was <0.02. Table 4A–C shows the output from the Transfind analysis of the gene sets in clusters 3, 4 and 5, respectively. The over-represented transcription factor binding sites were listed based on the order of significance. No significant enrichment of transcription factor binding sites was identified for the genes in clusters 1, 2 and 6. As indicated in Table 4A, for the genes in cluster 3, AP2 and E2F binding sites were highly significant with FDR<0.000058. Thirty-eight genes contained AP2 binding sites, which represented 6.9% of the genes in this cluster, whereas only 2.8% of the genes in the control set contained this binding site. The same number of genes contained E2F binding sites. However, only two genes (RBL1 and CBX7) contained both AP2 and E2F binding sites. The genes with putative AP2 binding sites were involved in diverse cellular signaling pathways. Another significant group of genes with AP2 sites was that involved in DNA, RNA and protein synthesis. The most important group of genes containing E2F binding sites, on the other hand, was that involved in cell cycle and DNA replication.

Table 4
Transfind analysis of over-represented transcription factor binding site motifs in the promoter region of genes in cluster 3 (A), cluster 4 (B) and cluster 5 (C).

Rank	TF matrix	p-value	FDR	Hits in positive set	Hits in negative set
A					
1	AP2_Q3	0.0000008	0.0000577	38 (6.934%)[a]	462 (2.789%)[b]
2	E2F_Q6_01	0.0000008	0.0000577	38 (6.934%)	462 (2.789%)
3	GC_high	0.0000008	0.0000577	38 (6.934%)	462 (2.789%)
4	AHRHIF_Q6	0.0000133	0.0007208	35 (6.387%)	465 (2.8075%)
5	E2F_02	0.0003661	0.0132402	31 (5.657%)	469 (2.831%)
6	SP1_Q4_01	0.0003661	0.0132402	31 (5.657%)	469 (2.831%)
B					
1	E2F_02	0.0000000	0.000000013	98 (7.413%)	402 (2.546%)
2	E2F_Q6_01	0.0000000	0.000000013	96 (7.262%)	404 (2.558%)
3	E2F_01	0.000000001	0.000000049	79 (5.976%)	421 (2.666%)
4	CREBATF_Q6	0.000001626	0.000070582	69 (5.22%)	431 (2.729%)
5	CpG_high	0.000001626	0.000070582	69 (5.22%)	431 (2.729%)
6	CREBP1CJUN_01	0.000077859	0.00241363	63 (4.766%)	437 (2.767%)
7	ATF4_Q2	0.000077859	0.00241363	63 (4.766%)	437 (2.767%)
8	ATF3_Q6	0.000245532	0.006660051	61 (4.614)	439 (2.78%)
9	CREBP1_Q2	0.000424329	0.009207931	60 (4.54%)	440 (2.786%)
10	CREB_Q2_01	0.000424329	0.009207931	60 (4.54%)	440 (2.786%)
11	ATF1_Q6	0.000719998	0.014203588	59 (4.46%)	441 (2.793%)
C					
1	SRF_01	0.000000833	0.000180679	59 (5.65%)	441 (2.74%)
2	NFκB65_01	0.000031438	0.003411022	54 (5.17%)	446 (2.78%)
3	EGR1_01	0.000116539	0.00842965	52 (4.98%)	448 (2.79%)

[a] The number and percentage of genes that contain specific transcription factor binding site among genes in the cluster.
[b] The number and percentage of genes that contain specific transcription factor binding site among all expressed genes.

Following the progression of the infection, more genes were activated at 24 hpi (cluster 4). Thus, it would be expected that a new set of transcription factors would be identified by Transfind. As shown in Table 4B, the E2F binding site was still the most overrepresented. Three variants of E2F binding sites were each present in 98, 97and 79 genes, respectively. There were however, overlaps between these variants. Taken together a total of 182 genes contained a putative E2F binding site. The transcription factor binding sites for several members of the ATF/CREB family, such as ATF1, ATF2 (CREBP1), CREB, ATF3 and ATF4 were also conspicuous. There were many overlaps between genes with these binding sites, and in total 137 genes contained a putative binding site for any of the transcription factors in the ATF/CREB family. As indicated by DAVID analysis, genes in cluster 4 were mainly involved in DNA replication, cell cycle, RNA and protein synthesis, or related metabolic processes.

A special set of transcription factor binding sites was identified in the promoter region of the differentially expressed genes in cluster 5 (Table 4C), which included genes that were down-regulated at 24 hpi. Transcription factor binding sites for SRF, NF-κB and EGR1 had the highest scores in this cluster. Fifty-nine genes (5.65%) contained SRF binding sites. SRF is a ubiquitous nuclear protein that binds to the serum response element (SRE) associated with a variety of genes including so-called immediate early genes like c-fos, fosB, junB, EGR1, EGR2 and HSP70. They play a pivotal role in transferring extracellular signals into specific nuclear responses (Chai and Tarnawski, 2002). Fifty-four genes (5.17%) harbored NF-κB binding sites. NF-κB mediates responses to stimuli such as stress and infection, and plays a key role in regulating the immune response to infection.

Expression of genes that encoded these key transcription factors was included in Table 5. Although the binding sites for AP2 and E2F were the most significant among the genes up-regulated from 12 hpi (in cluster 3), the expression profile of these two families of transcription factors was very different. Among AP2 family, only AP2A (or TFAP2A) was expressed, and its expression was decreasing with time after infection. Among eight E2F species, five E2F species were found to be expressed, and their expression increased dramatically following the progression of infection. For example, the expression of E2F2 was up 12 fold at 12 hpi and 87 fold at 24 hpi as compared with non-infected cell. The transcription of different members of the ATF/CREB family was very diverse; only ATF4 and ATF5 were up-regulated whereas the rest of them were either down-regulated or unchanged. Expression of both SRF and NF-κB decreased more than 2-fold, whereas EGR1 declined more than 17-fold. The decline in EGR1 expression might be a consequence of its dependence on SRF.

Control of cell growth and cell cycle

Deregulation of the host cell cycle is a prerequisite for a successful adenovirus infection in order to force the cell to enter the S phase. Binding of E1A to pRb results in the release of transcription factor E2F, which thereby activates transcription of genes required for the S phase induction and DNA replication. Our results showed that genes involved in the DNA replication and cell cycle regulation were the most significant up-regulated genes. Transfind analysis indicated that the most over-represented transcription factor binding site in the up-regulated genes either from 12 hpi (cluster 3) or 24 hpi (cluster 4) was E2F. In addition to the dramatic increase in E2F transcripts,

Table 5
Expression of putative transcription factors identified by Transfind.

Gene symbol	Fold change		Sequencing reads		
	Ad-12 hpi	Ad-24 hpi	Mock	Ad-12 hpi	Ad-24 hpi
TFAP2A	−2.5[a]	−3.6[b]	451.8	183.6	123.9
E2F1	3.1	12.1	127.2	389.6	1539.7
E2F2	12.8	87.9	3.9	50.1	344.3
E2F6	1.6	2.3	235.2	385.8	533.0
E2F7	−1.2	2.9	84.9	68.4	247.3
E2F8	2.1	13.2	11.9	25.3	156.8
E2F3	−1.3	−1.5	204.7	157.0	137.1
E2F4	−1.2	−1.3	1128.5	927.0	865.7
E2F5	1.6	−1.1	153.1	239.1	137.4
ATF1	−1.2	1.2	110.3	93.7	127.0
ATF2/CREBP1	1.1	−1.6	127.9	139.5	78.3
ATF3	1.0	1.1	258.2	266.7	279.0
ATF4	1.1	2.1	5458.4	5739.4	11,519.4
ATF5	1.4	2.0	455.8	649.5	902.7
ATF6	1.3	1.8	248.6	333.5	439.5
ATF7	1.1	−2.4	478.8	514.6	197.6
CREB1	1.0	1.1	115.5	118.5	132.8
SRF	−1.2	−2.3	944.6	787.4	406.0
NFKB2	−1.4	−2.4	2499.9	1760.7	1063.4
EGR1	−3.3	−17.1	871.3	267.4	51.0

[a] Fold change in gene expression (sequencing reads) between infected Ad-12 hpi and uninfected cells (mock).
[b] Fold change in gene expression (sequencing reads) between infected Ad-24 hpi and uninfected cells (mock).

expression of the partners, TFDP1 and TFDP2, was increased (Table 6). Furthermore, the key regulators of G1 to S phase progression, the cyclin-dependent kinases, CDK2 and CDK4, as well as their cyclin partners, CCNA2, CCNE1 and CCNE2, were also up-regulated. Moreover, the expression of the positive regulator of CDK2/CCNE, CDC25A, increased 26-fold, whereas their inhibitors CDKN1A (p21) and CDKN1C decreased significantly. Furthermore, expression of S-phase kinase-associated protein 2 (SKP2), a component of the E3 ligase that targets CDKN1A for degradation, increased. The activation of the cell cycle is thus massive.

As another over-represented transcription factor binding site in the up-regulated genes from 12 hpi (cluster 3), AP2 is known to act as tumor suppressor genes and regulates specific genes involved in cell cycle and cell death (Gee et al., 1999; Orso et al., 2008). The genes identified here that contained the AP2 transcription factor binding site were involved in various signaling pathways (MAK4P2, VAV2, POFUT1, PDE7A, SARM1, ARRB1, CMTM4, CACNA1H, ATP2A3, GNAZ, EFNA5 and PTPN3), cell cycle (RBL1 and CCNF) and DNA damage response (RBM38 and USP28). However, among five members of AP2 family, only AP2A was found to be expressed at a significant level, which decreased with time of infection. It could argue that the protein level of AP2A probably remained relatively stable during the early stage of infection. In the contrast to the E2F binding site which was present in the up-regulated genes both from 12 hpi and 24 hpi, the AP2 binding site was only significant in the genes up-regulated from 12 hpi, suggesting a role of AP2A during the very early stages of infection.

It could be speculated that one of the important conflicts between the host cell and the virus in cell cycle control was mediated by AP2 and E2F. Inhibition of the cell growth and cell cycle progression mediated by AP2 probably represents attempts by the anti-viral defense of the host during the early stage; whereas the activation of E2F by adenovirus E1A is a counterstrike by the virus. To overcome the loss of functional pRB due to the sequestration by E1A, the host cell increased expression of pRB and p107 (RBL1) 2.3 and 7.6 times, respectively. Another possible countermeasure was to up-regulate the expression of RBM38, an RNA-binding protein that binds to the 3′-utr of CDKN1A transcripts, thereby maintaining the stability of CDKN1A transcripts. It was noteworthy that both p107 and RBM38 contain AP2 binding sites. Furthermore, the increased expression of the negative regulators WEE1, CDKN2A and CDKN2C probably also represents an anti-viral effect.

In line with the activation of E2F, 219 up-regulated genes contained potential E2F binding sites within the promoter region (data not shown here). These genes included DNA polymerases (POLA1, POLD1, POLD3, POLE), replication factors (RFC2, 4 and 5), replication proteins RPA1 and RPA2, the minichromosome maintenance complex components (MCM2-9) and many histones (HIS2H4A and B, HIST2H2BE, HIST1H2BE 2BH, 2AK, 2BK and 2BJ, HIST1H4E and 4H, HIST1H3G), indicating that cellular DNA replication components were required to replicate the viral DNA efficiently. It is, on the other hand, difficult to see that the up-regulation of the histone genes would be in the interest of the virus as the viral DNA is covered by virus-encoded proteins.

Deregulation of cellular genes by the ATF/CREB transcription factor

The ATF/CREB transcription factor family appeared also to be important for up-regulation of many genes as revealed by Transfind (Table 4B). At least 5 different members of CREBP1, ATF4, ATF3, CREB and ATF1, were predicted to be involved in gene activation. However, when lists of target genes were compared, we found that the majority of the genes contained more than one binding site for ATF/CREB, allowing heterodimeric partners to bind and participate in the activation. In total, 137 target genes contained any type of ATF/CREB binding site. Members of the ATF/CREB family have diverse functions controlling cell proliferation and apoptosis. Our functional analysis indicated that the deregulated genes with ATF/CREB binding sites were involved in DNA metabolism (such as DNA mismatch repair, chromosomal structure, chromosome condensation and segregation) and RNA metabolism (such as transcription regulation and RNA processing). In addition, several members of ATF/CREB, like ATF2, ATF3 and ATF6, play a role in mediating stress response. Accordingly, several genes, which encoded negative regulators of the cell cycle such as WEE1, CDKN2A, CDKN2C and RB1 had ATF/CREB binding sites.

Activation of WNT signaling pathway

Many signaling pathways were targeted during adenovirus infection. Activation of Wnt signaling pathway appeared to be one of the most clear-cut. All detected receptors (FZD1, FZD5, FZD8 and FZD9) and co-receptors (LRP3, LRP4, LRP6 and LRP8) were up-regulated (Table 7), whereas the expression of inhibitors (MFRP, DKK1 and SFRP1) was down-regulated. Furthermore, the expression of Zinc finger protein SNAI2, a transcriptional repressor that binds to E-box motifs and represses E-cadherin transcription, decreased significantly. Notably, the expression of one well-known Wnt target gene, BIRC5 (Survivin), an anti-apoptotic protein, was up-regulated at 24 hpi. However, inhibition of the pathway was also seen, e.g. suppression of ligands WNT2, WNT5A and WNT5B and activation of APC2 expression, which targeted β-catenin for degradation. These effects were likely to be part of the cellular antiviral response. Activation of the Wnt pathway was rapid. Most of the deregulation had occurred at 12 hpi. So far, activation of the Wnt signaling pathway in adenovirus infected cells has only been shown at a transcriptional level. However, activation of the Wnt pathway has been demonstrated for other viruses such as a polyoma virus (JCV), Epstein-Barr virus (EBV) and Kaposi's sarcoma-associated herpesvirus (KSHV) (Enam et al., 2002; Fujimuro and Hayward, 2003; Morrison et al., 2003). Different strategies such as interaction with β-catenin (JCV), interaction with the negative regulator GSK-3β, which leads to stabilisation of the β-catenin (KSHV), or activation of the PI3K/Akt pathway which leads to inactivation of GSK3ß (EBV) have been seen.

Table 6
Expression of genes directly involved in cell cycle progression.

Gene symbol	Gene name	Fold change		Sequencing reads		
		Ad-12 hpi	Ad-24 hpi	Mock	Ad-12 hpi	Ad-24 hpi
CCNA2	Cyclin A2	−1.1[a]	3.5[b]	110.1	98.6	386.2
CCNB1IP1	Cyclin B1 interacting protein 1	1.0	2.2	1155.3	1172.1	2491.8
CCND1	Cyclin D1	−1.8	−7.3	11,835.0	6629.2	1619.9
CCNE1	Cyclin E1	5.4	6.3	206.9	1108.1	1303.8
CCNE2	Cyclin E2	8.4	22.3	24.4	205.3	543.2
CCNF	Cyclin F	2.1	1.9	126.7	262.1	240.2
CCNJL	Cyclin J-like	−1.2	−4.6	84.3	69.2	18.1
CCNL2	Cyclin L2	−1.3	−2.4	4408.6	3275.5	1803.1
CCNT1	Cyclin T1	2.2	2.2	96.8	215.9	209.1
CCNYL1	Cyclin Y-like 1	−1.1	−2.3	125.8	113.9	53.6
CDC123	Cell division cycle 123 homolog (*S. cerevisiae*)	1.0	2.0	517.8	528.9	1043.5
CDC2	Cyclin-dependent kinase-1	−1.1	7.1	206.1	196.3	1461.3
CDC20	Cell division cycle 20 homolog (*S. cerevisiae*)	−2.2	−1.2	420.6	188.0	357.4
CDC23	Cell division cycle 23	1.4	2.6	135.9	196.3	352.2
CDC25A	Cell division cycle 25 homolog A (*S. pombe*)	8.0	26.1	106.5	855.7	2781.2
CDC2L1	Cell division cycle 2-like 1	1.1	2.0	2438.4	2682.3	4957.6
CDC42EP2	CDC42 effector protein (Rho GTPase binding) 2	−1.1	−2.8	525.4	486.8	187.1
CDC42EP3	CDC42 effector protein (Rho GTPase binding) 3	−2.7	−8.5	1452.2	538.1	170.5
CDC45L	Cell division cycle 45 homolog	2.0	23.6	52.4	102.9	1233.8
CDC6	Cell division cycle 6 homolog (S. cerevisiae)	3.7	21.8	65.2	240.6	1423.3
CDC7	Cell division cycle 7 homolog (*S. cerevisiae*)	6.4	12.6	32.0	203.7	404.2
CDCA2	Cell division cycle associated 2	−1.4	2.3	32.6	23.1	76.0
CDCA3	Cell division cycle associated 3	−1.5	3.0	149.7	96.8	449.0
CDCA4	Cell division cycle associated 4	2.0	4.0	412.8	831.8	1635.4
CDCA5	Cell division cycle associated 5	1.2	10.7	145.9	180.9	1560.2
CDCA7	Cell division cycle associated 7	4.6	7.2	124.5	572.2	901.8
CDCA7L	Cell division cycle associated 7-like	2.1	5.1	388.0	822.8	1965.3
CDCA8	Cell division cycle associated 8	−1.7	2.9	149.5	87.7	436.4
CDK2	Cyclin-dependent kinase 2	2.4	6.1	503.6	1208.3	3092.0
CDK4	Cyclin-dependent kinase 4	1.2	2.7	1451.1	1796.7	3922.0
CDK5R1	Cyclin-dependent kinase 5. regulatory subunit 1 (p35)	6.8	6.1	24.1	163.4	147.4
CDK6	Cyclin-dependent kinase 6	−1.5	−3.8	503.7	331.4	134.0
CDK7	Cyclin-dependent kinase 7	−1.8	−3.9	315.7	176.0	80.0
CDKAL1	CDK5 regulatory subunit associated protein 1-like 1	1.3	2.9	48.1	63.0	140.4
CDKL3	Cyclin-dependent kinase-like 3	−1.1	5.1	31.2	29.3	159.3
CDKN1A	Cyclin-dependent kinase inhibitor 1A (p21. Cip1)	1.6	−2.7	14,596.5	23,466.6	5492.1
CDKN1C	Cyclin-dependent kinase inhibitor 1C (p57. Kip2)	−1.1	−3.3	162.3	143.4	49.1
CDKN2A	cyclin-dependent kinase inhibitor 2A	−1.1	2.0	1045.6	950.2	2134.1
CDKN2AIP	CDKN2A interacting protein	1.3	2.3	136.4	179.3	318.6
CDKN2BAS	CDKN2B antisense RNA 1	11.6	53.3	0.9	10.7	49.2
CDKN2C	Cyclin-dependent kinase inhibitor 2C (p18. inhibits CDK4)	1.1	2.0	179.2	200.3	364.6
CKS1B	CDC28 protein kinase regulatory subunit 1B	−1.3	1.7	290.1	218.7	494.6
RB1	Retinoblastoma 1	1.3	2.3	75.5	98.1	174.5
RBBP4	Retinoblastoma binding protein 4	1.1	2.4	656.1	710.9	1587.7
RBBP6	retinoblastoma binding protein 6	2.2	3.9	253.8	568.4	988.2
RBBP7	Retinoblastoma binding protein 7	1.2	2.4	755.2	900.9	1816.6
RBBP8	Retinoblastoma binding protein 8	1.8	4.5	270.1	485.8	1220.5
RBBP9	Retinoblastoma binding protein 9	1.9	2.5	38.1	73.9	96.1
RBL1	Retinoblastoma-like 1 (p107)	4.4	7.6	36.5	159.6	278.7
E2F1	E2F transcription factor 1	3.1	12.1	127.2	389.6	1539.7
E2F2	E2F transcription factor 2	12.8	87.9	3.9	50.1	344.3
E2F6	E2F transcription factor 6	1.6	2.3	235.2	385.8	533.0
E2F7	E2F transcription factor 7	−1.2	2.9	84.9	68.4	247.3
E2F8	E2F transcription factor 8	2.1	13.2	11.9	25.3	156.8
SKP2	S-phase kinase-associated protein 2 (p45)	3.8	10.3	181.8	693.9	1869.6
PCNA	Proliferating cell nuclear antigen	3.0	7.1	1547.9	4599.2	10,961.5
WEE1	WEE1 homolog (*S. pombe*)	2.7	4.0	188.4	500.7	753.7
TFDP1	Transcription factor Dp-1	1.6	3.6	1452.0	2364.7	5247.6
TFDP2	Transcription factor Dp-2 (E2F dimerization partner 2)	2.8	4.1	40.8	115.7	168.5

[a] Fold change in gene expression (sequencing reads) between infected Ad-12 hpi and uninfected cells (mock).
[b] Fold change in gene expression (sequencing reads) between infected Ad-24 hpi and uninfected cells (mock).

Suppression of TGF-β signaling pathways

DAVID annotation analysis showed that the down-regulated genes primarily were involved in various cellular signaling pathways including TGF-β, Rho, G-protein, Map kinase, STAT and NF-κB. Inhibition of TGF-β pathway was shown in our previous microarray study (Zhao et al., 2007). Here, a broader range of genes involved in TGF-β signaling pathway was identified (Table 8), which included the ligands of the TGF-β superfamily (BMP, GDFs and TGFBs), ligand agonist/antagonists, receptors, different SMADs (SMAD3, SMAD6, SMAD7), and the E3 ubiquitin-protein ligase (SMURF2), as well as SMAD binding proteins (ZEB2 and TGIF1).

Regulation of genes involved in TGF-β pathway during adenovirus infection seemed complicated, since both positive and negative regulators were both up- or down-regulated (Table 8). Examples were: 1) ligands of the superfamily included BMP, GDFs, and TGFBs; 2) several antagonists for BMP (NOG and BMPER), TGFB/GDF (GREM1, GREM2, DCN, THBS1, LTBP1 and LTBP2) and activin (INHBA, FST, FSTL1 and

Table 7
Expression of genes implicated in Wnt pathway and downstream targeted genes.

Function	Gene symbol	Gene name	Fold change		Sequencing reads		
			Ad-12 hpi	Ad-24 hpi	Mock	Ad-12 hpi	Ad-24 hpi
Ligand	WNT2	Wingless-type MMTV integration site family member 2	−1.7[a]	−4.1[b]	95.8	55.3	23.4
	WNT5A	Wingless-type MMTV integration site family. member 5A	1.0	−5.0	1058.5	1067.4	210.5
	WNT5B	Wingless-type MMTV integration site family. member 5B	−1.3	−5.6	4654.4	3634.3	830.7
	WNT7B	Wingless-type MMTV integration site family. member 7B	26.3	83.5	0.9	23.8	75.5
Receptor	FZD1	Frizzled homolog 1 (Drosophila)	3.5	1.5	182.2	631.4	277.2
	FZD5	Frizzled homolog 5 (Drosophila)	4.5	2.6	6.3	28.4	16.7
	FZD8	Frizzled homolog 8 (Drosophila)	2.7	−1.4	367.6	1010.2	266.5
	FZD9	Frizzled homolog 9 (Drosophila)	5.0	3.4	53.3	265.4	180.3
Coreceptor	LRP3	Low density lipoprotein receptor-related protein 3	1.5	2.5	303.1	452.3	768.7
	LRP4	Low density lipoprotein receptor-related protein 4	3.2	4.9	31.7	101.2	156.4
	LRP6	Low density lipoprotein receptor-related protein 6	2.1	1.9	77.2	160.3	145.6
	LRP8	Low density lipoprotein receptor-related protein 8	3.1	3.1	490.1	1533.6	1509.2
Inhibitor	MFRP	Membrane frizzled-related protein	−2.1	−2.4	157.2	75.1	66.2
	DKK1	Dickkopf homolog 1 (*Xenopus laevis*)	−4.3	−67.3	1974.5	461.8	29.3
	SFRP1	Secreted frizzled-related protein 1	1.1	−2.7	4030.2	4350.5	1518.3
Other	SNAI2	Snail homolog 2 (Drosophila)	−1.9	−5.1	379.0	199.4	74.4
	RRM2	Ribonucleotide reductase M2	1.2	9.2	362.6	452.4	3349.7
	APC2	Adenomatosis polyposis coli 2	4.3	7.9	14.2	61.7	112.0
	BIRC5	Baculoviral IAP repeat-containing 5	−1.8	3.9	604.4	333.1	2368.4

[a] Fold change in gene expression (sequencing reads) between infected Ad-12 hpi and uninfected cells (mock).
[b] Fold change in gene expression (sequencing reads) between infected Ad-24 hpi and uninfected cells (mock).

SFTL3) were all down-regulated whereas inhibins (INHBB and INHBE) were up-regulated; 3) the serine/threonine kinase receptors TGFBR1, TGFBR2, BMPR2, ACVR1 and ACVRL1 were down-regulated, while BMPR1B and ACVR2B were up-regulated; 4) all three detected SMADs, SMAD3, SMAD6 and SMAD7, were repressed, whereas expression of their antagonists, the E3 ubiquitin-protein ligases SMURF1 and SMURF2 was decreased. However, the net outcome was clearly that the TGF-β pathway was suppressed efficiently, supported by the facts that nearly all of the TGF-β target genes were down-regulated. It seemed that repression of genes that encode ligands, receptors and SMAD3, as well as the activation of genes encoding antagonists of ligands was mediated by the virus. The deregulation of genes implicated in the activation of the pathway most likely reflected the cellular defense. This included the down-regulation of genes encoding antagonists of ligands and the E3 ubiquitin ligase and the up-regulation of genes encoding ligands and their receptors. Our previous Western blot analysis showed that the expression of SMAD2 and SMAD1/3 at the protein level remained stable, whereas SMAD4 was increased until late after infection (Zhao et al., 2007). This might present another attempt of the host cell to counteract the inhibitory effect on the TGF-β pathway by adenovirus. Adenovirus-induced inhibition of TGF-β pathway was demonstrated in several earlier studies. E1A has been shown to block TGF-β-mediated induction of p21, p15 and JunB (Coussens et al., 1994b; Datto et al., 1997b; de Groot et al., 1995). E1A can also block growth inhibition by TGF-β through its binding to the hypophosphorylated pRb (Missero et al., 1991; Pietenpol et al., 1990) and SMAD proteins (Nishihara et al., 1999). Furthermore, the TGF-β receptor has been found to be down-regulated in E1A-transformed keratinocytes (Kim et al., 1997; Missero et al., 1991). Finally, the regulation of TGF-β pathway was also observed in our previous microarray study (Zhao et al., 2007). Further studies are needed to fully elucidate the mechanisms by which the adenovirus controls the pathway.

Inactivation of NF-κB pathway

Although the DAVID functional annotation analysis did not identify immune response genes as a significant group, the categories "regulation of signal transduction" and "apoptosis" (Table 3) included many genes in the NF-κB pathway. Furthermore, Transfind analysis showed that the NFκB binding site was the second most significant motif among the down-regulated genes, clearly indicating that the NF-κB pathway was suppressed. As shown in Table 9, expression of two of the key players of NF-κB pathway, NFKB2 and RelB, was down-regulated. The activity of NF-κB is primarily regulated by interaction with inhibitory IκB proteins and catalytic activation of the IκB kinase (IKK). The deregulation of IκB and IKK was, however, not clear-cut. Among 4 detected IκBs, one (NFKBIB) was up-regulated and three (NFKBIE, NFκBIA and BCL3) were down-regulated, whereas among three detected IκB kinases, two (IKBKE and IKBKG) were down-regulated and one (IKBKAP) was up-regulated, indicating a battle between the virus and its host. Examples of down-regulated NF-κB target genes were IL6, IL8, F3, BCL3, CCL2, TNFAIP3, THBS1 and INHBA.

A large variety of receptors that trigger NF-κB signaling were deregulated including genes involved in TNF mediated signaling. A diversity of TNF receptors was found to be both up and down-regulated (Table 10), such as receptors which contained a cytoplasmic death domain (TNFRSF10A, TNFRSF1A, TNFRSF25), receptors which contained a TNF-receptor associated factor (TRAF)-interacting motif in their cytoplasmic domain (TNFRSF1B, TNFRSF11A, TNFRSF12A, TNFRSF8 and TNFRSF19), as well as receptors which contained no signaling motif (TNFRSF11B) but competed with the other two groups of receptors for ligands. However, down-regulation of TNFRSF1A, a major receptor for the TNFα, and its downstream adaptor protein, TRADD, FADD, R1PK1 and IAP1, indicated suppression of the TNF signaling pathway. In contrast, the signaling mediated through TNF receptors with a TRAF-interacting motif was inconsistent as three out of 5 were up-regulated, whereas their adaptor proteins TRAF3 and TRAF1 were up- and down-regulated, respectively. In addition to NF-κB signaling, TNF signaling also leads to apoptosis and other inflammatory processes. Therefore, it is essential for the adenovirus to suppress this signaling pathway.

Complex deregulation of the apoptosis pathways

The occurrence of E1A induced p53-dependent apoptosis and E1B protein mediated suppression has been shown before (White, 2001). Our present study provided a comprehensive view of how cellular genes involved in apoptosis were deregulated. Both the TNF signaling pathway through the death receptor system and the stress induced Bcl inhibitory pathway were targeted. Expression of several Bcl2 family members and their transcriptional regulators changed

Table 8
Expression of genes implicated in TGF-β pathway and SMAD targeted genes.

Function	Gene symbol	Gene name	Fold change		Sequencing read		
			Ad-12 hpi	Ad-24 hpi	Mock	Ad-12 hpi	Ad-24 hpi
Ligand	BMP6	Bone morphogenetic protein 6	1.1[a]	2.1[b]	150.8	167.5	317.7
	GDF1	Growth differentiation factor 1	3.3	7.7	59.1	193.2	455.6
	TGFBRAP1	Transforming growth factor. beta receptor associated protein 1	1.8	2.1	284.1	515.3	586.1
	GDF15	Growth differentiation factor 15	−1.2	−4.5	857.3	689.7	189.3
	GDF5	Growth differentiation factor 5	−1.6	−16.5	268.4	163.7	16.3
	GDF6	Growth differentiation factor 6	−1.8	−7.0	83.0	46.9	11.9
Ligand agonist & ligand antagonists	BMPER	BMP binding endothelial regulator	−1.6	−27.4	197.6	122.6	7.2
	INHBB	Inhibin. beta B	1.4	5.1	14.4	20.3	72.9
	INHBE	Inhibin. beta E	1.9	20.2	5.1	9.8	102.8
	INHBA	Inhibin. beta A	−2.0	−5.5	1167.4	599.1	212.0
	NOG	Noggin	−2.6	−12.4	202.9	78.2	16.4
	GREM1	Gremlin 1	−1.4	−6.0	15,708.8	11,371.6	2614.9
	GREM2	Gremlin 2	−2.9	−19.6	339.6	116.0	17.3
	FST	Follistatin	−2.0	−6.5	8263.6	4059.5	1265.5
	FSTL1	Follistatin-like 1	−1.0	−2.2	7126.1	6861.0	3252.2
	FSTL3	Follistatin-like 3 (secreted glycoprotein)	1.2	−2.2	1348.8	1598.3	620.4
	THBS1	Thrombospondin 1	−3.4	−12.7	20,490.6	6006.6	1609.0
	LTBP1	Latent transforming growth factor beta binding protein 1	−1.0	−2.5	15,952.4	15,810.8	6501.1
	LTBP2	Latent transforming growth factor beta binding protein 2	1.1	−1.9	2908.4	3208.3	1554.9
	DCN	Decorin	−1.5	−2.2	90,841.8	62,202.2	41,234.0
Receptor	TGFBR1	Transforming growth factor. beta receptor 1	−2.4	−7.6	612.9	257.0	80.2
	TGFBR2	Transforming growth factor. beta receptor II	1.0	−2.4	2458.3	2491.9	1021.6
	BMPR1B	Bone morphogenetic protein receptor. type IB	2.2	5.7	4.8	10.5	27.2
	BMPR2	Bone morphogenetic protein receptor. type II	1.3	−2.3	179.0	227.2	78.6
	ACVR2B	Activin A receptor. type IIB	4.3	4.7	6.7	28.4	31.7
	ACVRL1	Activin A receptor type II-like 1	−1.3	−2.5	130.3	102.8	52.0
	ACVR1	Activin A receptor. type I	−1.3	−2.6	875.3	654.4	331.2
SMAD & SMAD regulator	SMAD3	SMAD family member 3	−1.3	−3.3	5920.9	4601.2	1818.6
	SMAD6	SMAD family member 6	−1.3	−7.7	273.3	210.3	35.7
	SMAD7	SMAD family member 7	−1.0	−3.2	289.2	279.2	89.5
	SMURF1	SMAD specific E3 ubiquitin protein ligase 1	−1.1	−2.0	629.3	585.2	311.2
	SMURF2	SMAD specific E3 ubiquitin protein ligase 2	−2.5	−9.9	1772.5	696.6	178.3
	TGIF1	TGFB-induced factor homeobox 1	−2.3	−4.6	2170.5	926.6	474.1
	TGIF2	TGFB-induced factor homeobox 2	2.2	1.8	92.3	201.1	165.4
	TGFBRAP1	Transforming growth factor. beta receptor associated protein 1	1.8	2.1	284.1	515.3	586.1
Targets	JUN	Jun proto-oncogene	−1.2	−4.9	1700.6	1376.1	347.7
	JUNB	Jun B proto-oncogene	1.6	−3.1	805.6	1259.3	261.0
	CDKN1A	Cyclin-dependent kinase inhibitor 1A (p21. Cip1)	1.6	−2.7	14,596.5	23,466.6	5492.1
	CDKN1C	Cyclin-dependent kinase inhibitor 1C (p57. Kip2)	−1.1	−3.3	162.3	143.5	49.1
	IL6	Interleukin 6 (interferon. beta 2)	−10.9	−156.1	681.7	62.6	4.4
	COL1A1	Collagen. type I. alpha 1	−1.0	−2.0	47,682.9	45,934.6	23,757.0
	IGFBP3	Insulin-like growth factor binding protein 3	−1.9	−9.2	5729.2	2983.7	624.6
	SERPINE1	Serpin peptidase inhibitor. clade E member 1	−2.1	−17.3	71,294.6	33,322.1	4114.2
	PDGFRB	Platelet-derived growth factor receptor. beta polypeptide	−1.0	−2.1	1183.8	1152.9	555.3
	TGFB1I1	Transforming growth factor beta 1 induced transcript 1	−1.8	−4.6	6962.3	3828.4	1503.7
	STAT1	Signal transducer and activator of transcription 1. 91 kDa	−1.4	−3.7	1395.6	1018.2	379.2
	DAB2	Disabled homolog 2. mitogen-responsive phosphoprotein	−3.3	−11.5	1383.1	420.7	120.7
	CDC25A	Cell division cycle 25 homolog A (*S. pombe*)	8.0	26.1	106.5	855.7	2781.2
	MYC	v-myc myelocytomatosis viral oncogene homolog (avian)	−1.5	−8.1	1026.0	708.7	126.7
	HIPK2	Homeodomain interacting protein kinase 2	1.1	−3.8	1103.2	1157.6	287.0
	ID1	Inhibitor of DNA binding 1. dominant negative helix–loop–helix protein	−2.6	−24.7	3067.0	1190.4	124.1
	ID2	Inhibitor of DNA binding 2. dominant negative helix–loop–helix protein	−1.6	−3.7	768.9	486.3	207.5

[a] Fold change in gene expression (sequencing reads) between infected Ad-12 hpi and uninfected cells (mock).
[b] Fold change in gene expression (sequencing reads) between infected Ad-24 hpi and uninfected cells (mock).

dramatically. As shown in Table 10, genes with both as pro- or anti-apoptotic functions were up- and down-regulated. BCL2L11 (pro-apoptotic) and BCL2 (anti-apoptotic) were up-regulated whereas BCL2L1 (anti-apoptotic) and BNIP3L (pro-apoptotic) were down-regulated. Besides, the pro-apoptotic gene BCLAF1, a transcriptional repressor of the BCL2 family was also up-regulated. In addition to the extrinsic apoptosis pathway, the intrinsic apoptosis pathway was deregulated. The sensors of cellular stress and the critical activators of apoptosis, the p53 family members, TP53 and TP73 were both activated. The up-regulation of TP73 was striking, from 29 fold at 12 hpi to more than 300 fold at 24 hpi. One of the important feature of TP73 is that it cannot be inactivated by E1B (Marin et al., 1998), but its transcriptional activation can be inhibited by E1A (Das et al., 2003). Apart from activating transcription of the majority of the p53-responsive genes, TP73 can also promote transcription of another set of genes (Fontemaggi et al., 2002). One of the example was the activation of JAG2 (ligand for Notch signaling pathway) gene.

Adenovirus-mediated suppression of STAT pathway

The signal transducer and activators of transcription (STAT) proteins have a crucial role in host defense. Expression of five out of 7 detectable of STATs (expression of STAT4 and STAT5A was very low in IMR-90 cell line as indicated by the number of sequencing reads) was down-regulated (Table 11). The down-regulation of STAT1, STAT2 and STAT6 was prominent. Consistently, expression of the interferon regulatory factor IRF9 was also down-regulated. STAT1, STAT2 and IRF9 form a heterotrimer complex, so called IFN-stimulated gene factor 3 (ISGF-3). The ISGF-3 complex binds to

Table 9
Deregulation of genes implicated in NF-kB pathway.

Function	Gene symbol	Gene name	Fold change		Sequencing reads		
			Ad-12 hpi	Ad-24 hpi	Mock	Ad-12 hpi	Ad-24 hpi
NF-κB	NFKB2	Nuclear factor of kappa light polypeptide gene enhancer in B-cells 2 (p49/p100)	−1.4[a]	−2.4[b]	2499.9	1760.7	1063.4
	RELB	v-rel reticuloendotheliosis viral oncogene homolog B	−1.8	−3.9	473.9	257.6	121.3
NF-κB inhibitor	NFKBIA	Nuclear factor of kappa light polypeptide gene enhancer in B-cells inhibitor. alpha	−1.3	−3.4	797.6	613.7	234.9
	NFKBIB	Nuclear factor of kappa light polypeptide gene enhancer in B-cells inhibitor. beta	1.8	4.8	748.1	1362.8	3570.8
	NFKBIE	Nuclear factor of kappa light polypeptide gene enhancer in B-cells inhibitor. epsilon	−3.3	−10.2	254.6	77.9	25.0
	BCL3	B-cell CLL/lymphoma 3	−1.2	−3.5	434.9	378.1	124.0
IκB kinase	IKBKAP	Inhibitor of kappa light polypeptide gene enhancer in B-cells. kinase complex-associated protein	2.1	2.4	126.3	269.6	303.8
	IKBKE	Inhibitor of kappa light polypeptide gene enhancer in B-cells. kinase epsilon	−1.8	−6.0	329.4	183.1	54.6
	IKBKG	Inhibitor of kappa light polypeptide gene enhancer in B-cells. kinase gamma	−1.5	−2.2	1641.7	1118.3	741.6
NF-κB regulator	NFKBIL2	Tonsoku-like. DNA repair protein	2.5	11.3	112.9	286.8	1276.3

[a] Fold change in gene expression (sequencing reads) between infected Ad-12 hpi and uninfected cells (mock).
[b] Fold change in gene expression (sequencing reads) between infected Ad-24 hpi and uninfected cells (mock).

ISRE DNA elements and induces expression of IFN target genes. This is the type I interferon (IFNα/β) pathway, which is very crucial in establishing an initial line of defense and is, therefore, the primary target of the viral immune evasion system (Goodbourn et al., 2000; Parisien et al., 2002). In addition, effectors and negative regulators were also differentially expressed. The effectors STAM and STAM2, adapter molecules, which can facilitate the transcription of specific target genes, were down-regulated. Members from all three major classes of negative regulators SOCS, PIAS, and PTPs were found to be deregulated. Most of them were down-regulated except SOCS4 and PIAS2. SOCS proteins block signaling from the receptor to the STATs, PIAS proteins block DNA binding of STATS, and PTPs dephosphorylate and deactivate JAK2, TYK2 and STAT5. Apparently, the adenovirus-mediated inhibition of the STAT pathway occurred at many steps. Host-mediated activation of the STAT pathway appeared to be limited, and mostly occurred through the activation of the negative regulators SOCS4 and PIAS2.

Previously we have studied and compared the changes in gene expression during infections with adenovirus type 2 and type 12 (Zhao et al., 2009). Ad2 replicates efficiently in IMR-90 cells and gives rise to a very strong cytopathic effect, as well as significant changes of cellular gene expression, whereas under the same conditions, Ad12 gives rise to a slower replication cycle and no significant cytopathic effect. In addition 4 times as many genes were differentially expressed in Ad2 infected cells as compared to Ad12-infected cells. One of the major differences was the deregulation of the STAT pathway. In Ad2-infected cells, expression of STAT3 and several cytokines was down-regulated. In Ad12-infected cells, in contrast, expression of STAT1, STAT2, as well as a numerous interferon-inducible genes, was up-regulated. Our present results showed that the STAT pathway was inhibited at multiple levels during Ad2 infection.

Deregulation of genes that encode cytokines and their receptors

Among various types of cytokines, deregulation of interleukins and their receptors was the most striking. The expression of all detected interleukins was rapidly reduced to a very low level (Table 11) from 12 hpi and continuing at 24 hpi. In contrast, the deregulation of interleukin receptors was inconsistent. Most of them, such as IL12RB2, IL17RB, IL17RD, IL6R, and IL20RB were up-regulated and significant activation occurred from 12 hpi, whereas only three, including IL1R, IL4R, and IL7R, were down-regulated which became significant after 24 hpi. The inconsistency of the deregulation of interleukins and their receptors could be interpreted as the results of the struggle between the virus and its host. Among differentially expressed cytokines, members of the IL-6 family (LIF, IL-11, IL-6, and CTF1) were noteworthy. All of them were down-regulated, IL6 more than 100-fold, whereas IL11 showed a 37-fold decrease. IL-6 is a multifunctional cytokine that plays a central role in host defense because of its wide range of immune and hematopoietic activities and its ability to induce the acute phase response. Many of the biological effects of IL-11 overlap those of IL-6. IL-11 is a multifunctional IL-6 type of cytokine with diverse biologic properties, including the ability to stimulate hematopoietic, thrombopoiesis and megakaryocytopoiesis. LIF is involved in the induction of hematopoietic differentiation in normal and myeloid leukemia cells. Furthermore, the IL-6 family binds to IL-6RB, which in turn activates the Janus kinase and finally, leads to the activation of STAT1 and STAT3. Thus, strong and rapid inhibition of cytokines might represent another mechanism for suppression of the host antiviral immune response. To overcome the loss of cytokines, the host cell seemed to activate some specific cytokine receptors which, however, did not seem to help.

Consistent with previous microarray studies

The temporal alternations of cellular gene expression following adenovirus infection of fibroblast cells have been studied by using microarray technology (Miller et al., 2007; Zhao et al., 2007). In IMR-90 cells, expression of over 460 cellular genes was changed during the early phase (from 6 to 24 hpi) of an adenovirus type 2 infection. In the present study, by using sequencing technology, 3791 cellular genes were identified as differentially expressed more than 2 fold, which was eight times more. In general, our sequencing results corroborated the earlier microarray results, but provided a great deal of additional information. Over 70% of the genes that were differentially expressed from 6 to 24 hpi identified by microarray technology were confirmed here. It is noteworthy that about 50% of the identified genes that have known functions were involved in control of cell cycle, cell growth, and antiviral response. The deregulation of genes involved in cell cycle regulation, such as CCNE1, CCNE2, CCNA2, CDCA5, CDK4, CDC45L, CDC25A, CDC6 could be detected in both studies. However, the list of genes in this functional category was much longer and much more quantitative in present study. Another consistent result was the activation of the Wnt pathway, the inhibition of TGF-β, STAT, NF-κB pathway, as well as the down-regulation of cytokines. In the TGF-β pathway, as many as 26 additional genes were discovered in the present study (see Table 8).

Miller et al. (2007) have studied alterations in the cellular transcription reprogram in human foreskin fibroblast cells after adenovirus type 5 infection by using microarrays with 44,000 reference points. They observed that the expression of about 2000 genes increased or decreased more than 2-fold. Cellular RNAs that were up-regulated early in infection were assigned important functions related to cellular proliferation included cell cycle check point proteins, DNA replication licensing proteins and cell cycle promoting transcription factors. Genes encoding proteins that mediate or regulate DNA replication were highly enriched, including genes encoding

Table 10
Deregulation of genes implicated in apoptosis.

Gene symbol	Gene name	Fold change		Sequencing reads		
		Ad-12 hpi	Ad-24 hpi	Mock	Ad-12 hpi	Ad-24 hpi
TNFSF4	Tumor necrosis factor (ligand) superfamily, member 4	−5.0[a]	−15.5[b]	315.1	63.0	20.3
EDA	Ectodysplasin A	37.2	80.2	0.7	26.6	57.4
TNFRSF1A	Tumor necrosis factor receptor superfamily. member 1A	−1.2	−2.7	1439.4	1171.5	535.5
TNFRSF25	Tumor necrosis factor receptor superfamily. member 25	1.1	−2.1	588.2	632.9	283.2
TNFRSF10A	Tumor necrosis factor receptor superfamily. member 10a	2.6	6.9	33.9	87.2	235.4
TNFRSF1B	Tumor necrosis factor receptor superfamily. member 1B	1.5	2.1	207.8	306.3	433.5
TNFRSF11A	Tumor necrosis factor receptor superfamily. member 11a. NFKB activator	11.4	86.1	0.3	3.2	24.4
TNFRSF8	Tumor necrosis factor receptor superfamily. member 8	4.7	27.0	6.1	29.0	165.7
TNFRSF12A	Tumor necrosis factor receptor superfamily. member 12A	−2.0	−6.3	7154.4	3525.6	1144.0
TNFRSF11B	Tumor necrosis factor receptor superfamily. member 11b	−5.2	−19.4	2460.1	470.6	126.6
TRADD	TNFRSF1A-associated via death domain	−1.2	−2.9	248.9	214.5	85.3
FADD	Fas (TNFRSF6)-associated via death domain	−1.3	−2.5	785.7	597.5	312.0
TRAF1	TNF receptor-associated factor 1	−2.2	−2.8	83.5	38.6	29.9
TRAF3	TNF receptor-associated factor 3	1.4	2.4	777.5	1092.9	1857.3
TRAF3IP2	TRAF3 interacting protein 2	−1.6	−3.2	580.7	364.7	178.7
TRAIP	TRAF interacting protein	−1.1	3.5	42.8	40.6	149.8
TRAP1	TNF receptor-associated protein 1	1.4	2.8	801.7	1148.4	2260.7
RIPK1	Receptor (TNFRSF)-interacting serine–threonine kinase 1	1.3	−2.0	204.5	271.3	100.6
DEDD	Death effector domain containing	−1.2	−2.3	1069.4	867.6	458.9
DEDD2	Death effector domain containing 2	−1.4	−2.6	352.0	259.0	137.5
TP53	Tumor protein p53	1.0	1.9	2442.9	2392.5	4733.4
TP73	Tumor protein p73	29.3	311.6	4.8	140.6	1494.0
CFLAR	CASP8 and FADD-like apoptosis regulator	−1.6	−4.0	805.6	504.5	200.1
CASP1	Caspase 1. apoptosis-related cysteine peptidase	−2.1	−3.9	917.2	447.2	236.8
CASP4	Caspase 4. apoptosis-related cysteine peptidase	−2.0	−3.2	2477.8	1262.3	772.6
CASP7	Caspase 7. apoptosis-related cysteine peptidase	1.7	2.2	287.0	499.6	619.6
CASP8AP2	Caspase 8 associated protein 2	2.5	2.1	156.2	392.7	334.6
BCL10	B-cell CLL/lymphoma 10	−1.8	−3.3	100.2	55.3	30.5
BCL2	B-cell CLL/lymphoma 2	7.4	10.8	8.0	59.3	86.8
BCL2L1	BCL2-like 1	−1.7	−4.5	2497.7	1499.4	558.8
BCL2L11	BCL2-like 11 (apoptosis facilitator)	14.1	28.4	25.4	359.5	722.1
BCLAF1	BCL2-associated transcription factor 1	1.1	2.6	706.7	776.0	1814.1
BAG3	BCL2-associated athanogene 3	−1.8	−2.3	1802.8	980.8	777.8
BNIP3L	BCL2/adenovirus E1B 19 kDa interacting protein 3-like	−2.4	−3.8	497.1	207.2	131.6

[a] Fold change in gene expression (sequencing reads) between infected Ad-12 hpi and uninfected cells (mock).
[b] Fold change in gene expression (sequencing reads) between infected Ad-24 hpi and uninfected cells (mock).

subunits of DNA polymerase, MCM complex components, and proteins that regulate spindle formation, chromosome condensation, segregation etc. Furthermore, among down-regulated genes, those involved in cell communication, signal transduction and development were also significant during the adenovirus type 5 infection. Thus the present results are consistent with this study and our own microarray studies (Zhao et al., 2007).

In the present study we have used state of the art technologies to study the changes in host cell gene expression that were caused by an adenovirus infection. The data obtained was much more precise and quantitative compared to the studies reported by us and others (Miller et al., 2007; Zhao et al., 2007). In addition, a number of bioinformatics tools have become available since earlier reports and these were applied to the huge data set that our study generated. A weak point is that RNA was analyzed at only two time points after infection due to the high cost of sequence analysis. Another shortcoming is the difficulty to define whether deregulation of gene expression is caused by viral gene products or reflect the host cell responses to the infection. Nonetheless, our RNA sequencing studies are one step further towards the understanding of interaction between adenovirus and its host cell. Insights from such studies shed light on how viruses take control of the infected cell and should ultimately identify new general targets for the design of anti-viral substances. Furthermore, our high quality sequence data base provides a valuable resource for studying gene regulation and gene function when novel analytical tools become available.

Materials and methods

Cell culture and adenovirus infection

Human primary lung fibroblast cells (IMR-90) (American Type Culture Collection) were cultured in Eagle's minimum essential medium (MEM) with Earle's salt and GlutaMAX™ supplemented with 10% fetal bovine serum, 100 U/ml penicillin, 0.1 mg/ml streptomycin, 0.1 mM nonessential amino acids, 1.5 g/l sodium bicarbonate and 1.0 mM sodium pyruvate. The IMR-90 cells were synchronized by growth inhibition through cultivation for two days after confluence, as described previously (Zhao et al., 2007). Synchronized monolayer cells were mock-infected or infected with Ad2 at a multiplicity of 100 fluorescence-forming units (FFU) per cell (Philipson, 1961) in serum-free medium. After 1 h adsorption at 37 °C, the medium was replaced with MEM containing 10% FBS and incubated at 37 °C. Infected cells were collected at 6, 12, 24, 36 and 48 hours post infection (hpi). Mock-infected cells were collected at 6 hpi. However, only 12 and 24 hpi as well as mock infection were subjected to the sequencing analysis. According to our previous experiments, no dramatic change was observed between 6 and 48 h in mock-infected cells.

RNA extraction, cDNA library preparation and sequencing

Total RNA from adenovirus or mock-infected IMR-90 was extracted using TRIZOL Reagent (Invitrogen). The quantity and quality of the RNA

Table 11
Deregulation of genes involved in STAT signaling pathway and genes encoded cytokines and cytokine receptors/regulators.

Function	Gene symbol	Gene name	Fold change		Sequencing reads		
			Ad-12 hpi	Ad-24 hpi	Mock	Ad-12 hpi	Ad-24 hpi
STAT signaling	STAT1	Signal transducer and activator of transcription 1	−1.4[a]	−3.7[b]	1395.6	1018.2	379.2
	STAT2	Signal transducer and activator of transcription 2	−1.5	−4.9	330.0	225.3	67.7
	STAT3	Signal transducer and activator of transcription 3	−1.2	−1.9	1726.4	1470.6	913.3
	STAT6	Signal transducer and activator of transcription 6	−1.3	−2.4	871.4	645.8	357.1
	STAT5A	Signal transducer and activator of transcription 5A	1.4	−1.2	62.8	86.3	51.0
	STAT5B	Signal transducer and activator of transcription 5B	−1.1	−1.5	209.8	194.6	141.9
	STAT4	Signal transducer and activator of transcription 4	−1.5	1.1	4.5	3.0	5.1
	IRF9/p48	Interferon regulatory factor 9	−1.5	−4.0	254.9	175.5	63.1
	SOCS2	Suppressor of cytokine signaling 2	−2.3	−3.0	244.5	107.9	82.3
	SOCS4	Suppressor of cytokine signaling 4	2.2	7.0	95.8	211.4	667.4
	SOCS5	Suppressor of cytokine signaling 5	−1.5	−5.0	751.4	510.9	149.4
	PIAS2	Protein inhibitor of activated STAT. 2	1.4	2.0	176.9	250.5	355.1
	PIAS3	Protein inhibitor of activated STAT. 3	−1.2	−3.7	671.8	564.4	179.7
	PTPN1	Protein tyrosine phosphatase. non-receptor type 1	−1.8	−2.1	679.6	384.0	318.6
	STAM	Signal transducing adaptor molecule (SH3 domain and ITAM motif) 1	−1.83	−2.27	249.02	135.83	109.65
	STAM2	Signal transducing adaptor molecule (SH3 domain and ITAM motif) 2	−1.18	−3.05	128.49	109.30	42.11
Cytokines. Cytokine receptors & regulators	IL6	Interleukin 6 (interferon. beta 2)	−10.9	−156.1	681.7	62.6	4.4
	IL8	Interleukin 8	−4.0	−20.4	238.9	59.8	11.7
	IL11	Interleukin 11	−2.6	−37.0	1033.3	404.4	28.0
	IL15	Interleukin 15	−4.2	−7.9	95.4	22.5	12.1
	IL12A	Interleukin 12A	−3.6	−12.6	135.5	38.2	10.8
	LIF	Leukemia inhibitory factor	−5.4	−8.3	4313.2	801.9	520.7
	IFNA1	Interferon. alpha 1	−17.0	−71.0	71.7	17.7	0.0
	IFNE	Interferon. epsilon	−4.0	−50.0	131.6	32.9	2.6
	CCL2	Chemokine (C-C motif) ligand 2	−19.0	−219.7	6090.8	321.3	27.7
	CTF1	Cardiotrophin 1	−2.4	−7.9	282.1	118.7	35.7
	CXCL16	Chemokine (C-X-C motif) ligand 16	3.9	8.0	26.7	103.2	212.8
	IL12RB2	Interleukin 12 receptor. beta 2	13.4	118.2	0.4	5.9	51.8
	IL17RB	Interleukin 17 receptor B	4.1	14.9	20.8	85.1	310.8
	IL17RD	Interleukin 17 receptor D	3.5	1.9	9.9	34.4	18.9
	IL1R1	Interleukin 1 receptor. type I	−1.2	−2.0	273.3	232.0	135.5
	IL1RAP	Interleukin 1 receptor accessory protein	−1.6	−2.4	233.5	144.2	97.2
	IL20RB	Interleukin 20 receptor beta	1.1	5.8	9.5	10.7	55.0
	IL4R	Interleukin 4 receptor	−1.2	−2.3	1100.1	928.5	482.9
	IL6R	Interleukin 6 receptor	4.6	5.5	23.6	109.3	130.7
	IL7R	Interleukin 7 receptor	−1.7	−12.3	741.7	445.1	60.2
	LIFR	Leukemia inhibitory factor receptor alpha	2.0	1.7	51.8	104.1	89.9
	CXCR4	Chemokine (C-X-C motif) receptor 4	11.8	63.0	0	11.8	62.9
	CRLF3	Cytokine receptor-like factor 3	1.2	2.1	72.5	86.7	154.1
	IRAK2	Interleukin-1 receptor-associated kinase 2	−1.2	−2.6	118.8	98.8	45.0
	IRAK3	Interleukin-1 receptor-associated kinase 3	5.4	9.4	6.8	36.7	63.7
	IRF5	Interferon regulatory factor 5	3.1	7.4	7.9	24.0	58.3
	IFI30	Interferon. gamma-inducible protein 30	2.0	5.6	39.4	78.8	222.6
	CNTF	Ciliary neurotrophic factor	1.5	6.2	18.2	27.5	113.3

[a] Fold change in gene expression (sequencing reads) between infected Ad-12 hpi and uninfected cells (mock).
[b] Fold change in gene expression (sequencing reads) between infected Ad-24 hpi and uninfected cells (mock).

were assessed using the RNA 6000 Nano LabChip kit and a Bioanalyzer 400 (Agilent Technologies). The cDNA libraries were prepared using Illumina mRNA Seq sample preparation kits (RS-100-0801) according to the manufacturer's protocol (Part # 1004898 Rev A). Single-end sequencing was performed using an Illumina Genome Analyzer II instrument.

Data collection and mapping of reads

The three sets of reads (mock, Ad-12 h and Ad-24 h) from the Illumina sequencing were aligned to both a human reference genome [GRCh37/hg19] and an adenovirus reference genome [http://www.ncbi.nlm.nih.gov/nuccore/AC_000007, 12/2008] using the software Bowtie (Langmead et al., 2009) and using the default parameters. The resulting alignments were loaded into R [R Development Core Team (2010). *R: A language and environment for statistical computing*. R Foundation for Statistical Computing, Vienna, Austria. ISBN 3-900051-07-0, URL http://www.R-project.org/] and all the reads that mapped to exons according to gene annotations (RefSeq Genes) from UCSC Genome Browser (Kent et al., 2002) were extracted. All overlapping splice variants of genes were merged and the gene annotations comprised 23,162 unique genes. The read counts (the number of mapped reads) for individual exons were summarized to read counts for the corresponding genes. All R code used in the analysis is available upon request.

Data analysis

The proportionality test function in the stats package to R was applied to each gene using the read-count in each data set and the total size of each data set. This function calculates the probability that the gene has the same proportion of reads at the three time points, i.e. that it is not differentially expressed. The reads for genes from different time points were normalized in regard to the time points total data set size. To avoid distortion of this analysis due to the large portion of adenovirus reads in the 24 hpi sample, the human and adenovirus genomes were analyzed separately. Differentially expressed genes were identified as significant if their expressions were more than 2-fold changes and with a proportionality test p-value $<1E^{-20}$.

Expression analysis

The web based software DAVID (Huang da et al., 2009a,b) was used to perform a gene ontology enrichment analysis of the differentially

expressed genes. The annotated genes from the RefSeq data set were used as background. This analysis searched for biochemical pathways and gene ontologies that were overrepresented in our sample, compared to a random sample of equal size from the background list.

A k-means clustering based on the normalized expression profile of each gene was also made with the program Genesis (Sturn et al., 2002). The normalization was done to get a rough image of the shape of the expression profile. The clusters were then subjected to ontology enrichment and overrepresented transcription factor binding motifs analyses (as described below).

Transcription factor binding sites

Transfind (http://transfind.sys-bio.net/) looks for areas in the promoter region of a set of genes that are likely to bind to known transcription factors (TFs) (Kielbasa et al., 2010). If all the genes in a set show an over representation of the same TF, it is likely that they are all regulated by that TF. This analysis was applied to the gene set after a clustering based on expression profile.

Acknowledgments

Sequencing was performed at the SNP&SEQ Technology Platform in Uppsala, supported by Uppsala University and University Hospital, the Knut and Alice Wallenberg Foundation and the Swedish Research Council (VR-KFI). We thank Kristina Larsson for excellent sequencing, Markus Rasmussen for support of data analysis, Catharina Svensson for critical reading of manuscript, Lu Lu for cell culture and virus infection. This work was supported by the Kjell and Märta Beijer Foundation.

References

Ames, R.S., Holskin, B., Mitcho, M., Shalloway, D., Chen, M.J., 1990. Induction of sensitivity to the cytotoxic action of tumor necrosis factor alpha by adenovirus E1A is independent of transformation and transcriptional activation. J. Virol. 64 (9), 4115–4122.

Arany, Z., Newsome, D., Oldread, E., Livingstone, D.M., Eckner, R., 1995. A family of transcriptional adaptor proteins targeted by the E1A oncoprotein. Nature 374, 81–84.

Bagchi, S., Raychaudhuri, P., Nevins, J.R., 1990. Adenovirus E1A proteins can dissociate heteromeric complexes involving the E2F transcription factor: a novel mechanism for E1A trans-activation. Cell 62 (4), 659–669.

Bannister, A.J., Kouzarides, T., 1995. CBP-induced stimulation of c-Fos activity is abrogated by E1A. EMBO J. 14 (19), 4758–4762.

Bayley, S.T., Mymryk, J.S., 1994. Adenovirus E1A proteins and transformation (Review). Int. J. Oncol. 5 (3).

Bennett, E.M., Bennink, J.R., Yewdell, J.W., Brodsky, F.M., 1999. Cutting edge: adenovirus E19 has two mechanisms for affecting class I MHC expression. J. Immunol. 162 (9), 5049–5052.

Burgert, H.G., Maryanski, J.L., Kvist, S., 1987. "E3/19K" protein of adenovirus type 2 inhibits lysis of cytolytic T lymphocytes by blocking cell-surface expression of histocompatibility class I antigens. Proc. Natl. Acad. Sci. U. S. A. 84 (5), 1356–1360.

Chai, J., Tarnawski, A.S., 2002. Serum response factor: discovery, biochemistry, biological roles and implications for tissue injury healing. J. Physiol. Pharmacol. 53 (2), 147–157.

Chen, M.J., Holskin, B., Strickler, J., Gorniak, J., Clark, M.A., Johnson, P.J., Mitcho, M., Shalloway, D., 1987. Induction by E1A oncogene expression of cellular susceptibility to lysis by TNF. Nature 330 (6148), 581–583.

Chinnadurai, G., 2004. Modulation of oncogenic transformation by the human adenovirus E1A C-terminal region. Curr. Top. Microbiol. Immunol. 273, 139–161.

Chow, L.T., Broker, T.R., Lewis, J.B., 1979. Complex splicing patterns of RNAs from the early regions of adenovirus-2. J. Mol. Biol. 134 (2), 265–303.

Cobrinik, D., 1996. Regulatory interactions among E2Fs and cell cycle control proteins. Curr. Top. Microbiol. Immunol. 208, 31–61.

Cook, J.L., Walker, T.A., Worthen, G.S., Radke, J.R., 2002. Role of the E1A Rb-binding domain in repression of the NF-kappa B-dependent defense against tumor necrosis factor-alpha. Proc. Natl. Acad. Sci. U. S. A. 99 (15), 9966–9971.

Coussens, L.M., Yokoyama, K., Chiu, R., 1994a. Transforming growth factor beta 1-mediated induction of junB is selectively inhibited by expression of Ad.12-E1A. J. Cell. Physiol. 160 (3), 435–444.

Coussens, L.M., Yokoyama, K., Chiu, R., 1994b. Transforming growth factor beta 1-mediated induction of junB is selectively inhibited by expression of Ad.12-E1A. J. Cell. Physiol. 160 (3), 435–444.

Cuesta, R., Xi, Q., Schneider, R.J., 2000. Adenovirus-specific translation by displacement of kinase Mnk1 from cap-initiation complex eIF4F. EMBO J. 19 (13), 3465–3474.

Das, S., El-Deiry, W.S., Somasundaram, K., 2003. Regulation of the p53 homolog p73 by adenoviral oncogene E1A. J. Biol. Chem. 278 (20), 18313–18320.

Datto, M.B., Hu, P.P., Kowalik, T.F., Yingling, J., Wang, X.F., 1997a. The viral oncoprotein E1A blocks transforming growth factor beta-mediated induction of p21/WAF1/Cip1 and p15/INK4B. Mol. Cell. Biol. 17 (4), 2030–2037.

Datto, M.B., Hu, P.P., Kowalik, T.F., Yingling, J., Wang, X.F., 1997b. The viral oncoprotein E1A blocks transforming growth factor beta-mediated induction of p21/WAF1/Cip1 and p15/INK4B. Mol. Cell. Biol. 17 (4), 2030–2037.

de Groot, R.P., Kranenburg, O., de Wit, L., van den Eijnden-van Raaij, J., Mummery, C., van der Eb, A.J., Zantema, A., 1995. Adenovirus E1A antagonizes both negative and positive growth signals elicited by transforming growth factor beta 1. Cell Growth Differ. 6 (5), 531–540.

Debbas, M., White, E., 1993. Wild-type p53 mediates apoptosis by E1A, which is inhibited by E1B. Genes Dev. 7 (4), 546–554.

Deleu, L., Shellard, S., Alevizopoulos, K., Amati, B., Land, H., 2001. Recruitment of TRRAP required for oncogenic transformation by E1A. Oncogene 20 (57), 8270–8275.

Duerksen-Hughes, P., Wold, W.S., Gooding, L.R., 1989. Adenovirus E1A renders infected cells sensitive to cytolysis by tumor necrosis factor. J. Immunol. 143 (12), 4193–4200.

Enam, S., Del Valle, L., Lara, C., Gan, D.D., Ortiz-Hidalgo, C., Palazzo, J.P., Khalili, K., 2002. Association of human polyomavirus JCV with colon cancer: evidence for interaction of viral T-antigen and beta-catenin. Cancer Res. 62 (23), 7093–7101.

Farley, D.C., Brown, J.L., Leppard, K.N., 2004. Activation of the early-late switch in adenovirus type 5 major late transcription unit expression by L4 gene products. J. Virol. 78 (4), 1782–1791.

Farrow, S.N., White, J.H., Martinou, I., Raven, T., Pun, K.T., Grinham, C.J., Martinou, J.C., Brown, R., 1995. Cloning of a bcl-2 homologue by interaction with adenovirus E1B 19K. Nature 374 (6524), 731–733.

Ferrari, R., Pellegrini, M., Horwitz, G.A., Xie, W., Berk, A.J., Kurdistani, S.K., 2008. Epigenetic reprogramming by adenovirus e1a. Science 321 (5892), 1086–1088.

Flint, J., Shenk, T., 1997. Viral transactivating proteins. Annu. Rev. Genet. 31, 177–212.

Fontemaggi, G., Kela, I., Amariglio, N., Rechavi, G., Krishnamurthy, J., Strano, S., Sacchi, A., Givol, D., Blandino, G., 2002. Identification of direct p73 target genes combining DNA microarray and chromatin immunoprecipitation analyses. J. Biol. Chem. 277 (45), 43359–43368.

Friedman, J.M., Horwitz, M.S., 2002. Inhibition of tumor necrosis factor alpha-induced NF-kappa B activation by the adenovirus E3-10.4/14.5K complex. J. Virol. 76 (11), 5515–5521.

Fuchs, M., Gerber, J., Drapkin, R., Sif, S., Ikura, T., Ogryzko, V., Lane, W.S., Nakatani, Y., Livingston, D.M., 2001. The p400 complex is an essential E1A transformation target. Cell 106 (3), 297–307.

Fujimuro, M., Hayward, S.D., 2003. The latency-associated nuclear antigen of Kaposi's sarcoma-associated herpesvirus manipulates the activity of glycogen synthase kinase-3beta. J. Virol. 77 (14), 8019–8030.

Gee, J.M., Robertson, J.F., Ellis, I.O., Nicholson, R.I., Hurst, H.C., 1999. Immunohistochemical analysis reveals a tumour suppressor-like role for the transcription factor AP-2 in invasive breast cancer. J. Pathol. 189 (4), 514–520.

Goodbourn, S., Didcock, L., Randall, R.E., 2000. Interferons: cell signalling, immune modulation, antiviral response and virus countermeasures. J. Gen. Virol. 81 (Pt 10), 2341–2364.

Granberg, F., Svensson, C., Pettersson, U., Zhao, H., 2006. Adenovirus-induced alterations in host cell gene expression prior to the onset of viral gene expression. Virology 353 (1), 1–5.

Han, J., Sabbatini, P., Perez, D., Rao, L., Modha, D., White, E., 1996. The E1B 19K protein blocks apoptosis by interacting with and inhibiting the p53-inducible and death-promoting Bax protein. Genes Dev. 10 (4), 461–477.

Hartman, Z.C., Kiang, A., Everett, R.S., Serra, D., Yang, X.Y., Clay, T.M., Amalfitano, A., 2007. Adenovirus infection triggers a rapid, MyD88-regulated transcriptome response critical to acute-phase and adaptive immune responses in vivo. J. Virol. 81 (4), 1796–1812.

Hayes, B.W., Telling, G.C., Myat, M.M., Williams, J.F., Flint, S.J., 1990. The adenovirus L4 100-kilodalton protein is necessary for efficient translation of viral late mRNA species. J. Virol. 64 (6), 2732–2742.

Huang da, W., Sherman, B.T., Lempicki, R.A., 2009a. Bioinformatics enrichment tools: paths toward the comprehensive functional analysis of large gene lists. Nucleic Acids Res. 37 (1), 1–13.

Huang da, W., Sherman, B.T., Lempicki, R.A., 2009b. Systematic and integrative analysis of large gene lists using DAVID bioinformatics resources. Nat. Protoc. 4 (1), 44–57.

Jennings-Gee, J.E., Tsuji, Y., Pietsch, E.C., Moran, E., Mymryk, J.S., Torti, F.M., Torti, S.V., 2006. Coordinate inhibition of cytokine-mediated induction of ferritin H, manganese superoxide dismutase, and interleukin-6 by the adenovirus E1A oncogene. J. Biol. Chem. 281 (24), 16428–16435.

Johansson, C., Zhao, H., Bajak, E., Granberg, F., Pettersson, U., Svensson, C., 2005. Impact of the interaction between adenovirus E1A and CtBP on host cell gene expression. Virus Res. 113, 51–63.

Jones, N., 1995. Transcriptional modulation by the adenovirus E1A gene. Curr. Top. Microbiol. Immunol. 199 (Pt 3), 59–80.

Kent, W.J., Sugnet, C.W., Furey, T.S., Roskin, K.M., Pringle, T.H., Zahler, A.M., Haussler, D., 2002. The human genome browser at UCSC. Genome Res. 12 (6), 996–1006.

Kielbasa, S.M., Klein, H., Roider, H.G., Vingron, M., Bluthgen, N., 2010. TransFind—predicting transcriptional regulators for gene sets. Nucleic Acids Res. 38 (Web Server issue), W275–W280.

Kim, D.H., Chang, J.H., Lee, K.H., Lee, H.Y., Kim, S.J., 1997. Mechanism of E1A-induced transforming growth factor-beta (TGF-beta) resistance in mouse keratinocytes involves repression of TGF-beta type II receptor transcription. J. Biol. Chem. 272 (1), 688–694.

Langmead, B., Trapnell, C., Pop, M., Salzberg, S.L., 2009. Ultrafast and memory-efficient alignment of short DNA sequences to the human genome. Genome Biol. 10 (3), R25.
Lomonosova, E., Subramanian, T., Chinnadurai, G., 2005. Mitochondrial localization of p53 during adenovirus infection and regulation of its activity by E1B-19K. Oncogene 24 (45), 6796–6808.
Lowe, S.W., Ruley, H.E., 1993. Stabilization of the p53 tumor suppressor is induced by adenovirus 5 E1A and accompanies apoptosis. Genes Dev. 7 (4), 535–545.
Marin, M.C., Jost, C.A., Irwin, M.S., DeCaprio, J.A., Caput, D., Kaelin Jr., W.G., 1998. Viral oncoproteins discriminate between p53 and the p53 homolog p73. Mol. Cell. Biol. 18 (11), 6316–6324.
Miller, D.L., Myers, C.L., Rickards, B., Coller, H.A., Flint, S.J., 2007. Adenovirus type 5 exerts genome-wide control over cellular programs governing proliferation, quiescence, and survival. Genome Biol. 8 (4), R58.
Miller, D.L., Rickards, B., Mashiba, M., Huang, W., Flint, S.J., 2009. The adenoviral E1B 55-kilodalton protein controls expression of immune response genes but not p53-dependent transcription. J. Virol. 83 (8), 3591–3603.
Missero, C., Filvaroff, E., Dotto, G.P., 1991. Induction of transforming growth factor beta 1 resistance by the E1A oncogene requires binding to a specific set of cellular proteins. Proc. Natl. Acad. Sci. U. S. A. 88 (8), 3489–3493.
Morrison, J.A., Klingelhutz, A.J., Raab-Traub, N., 2003. Epstein-Barr virus latent membrane protein 2A activates beta-catenin signaling in epithelial cells. J. Virol. 77 (22), 12276–12284.
Nishihara, A., Hanai, J., Imamura, T., Miyazono, K., Kawabata, M., 1999. E1A inhibits transforming growth factor-beta signaling through binding to Smad proteins. J. Biol. Chem. 274 (40), 28716–28723.
Orso, F., Penna, E., Cimino, D., Astanina, E., Maione, F., Valdembri, D., Giraudo, E., Serini, G., Sismondi, P., De Bortoli, M., Taverna, D., 2008. AP-2alpha and AP-2gamma regulate tumor progression via specific genetic programs. FASEB J. 22 (8), 2702–2714.
Parisien, J.P., Lau, J.F., Rodriguez, J.J., Ulane, C.M., Horvath, C.M., 2002. Selective STAT protein degradation induced by paramyxoviruses requires both STAT1 and STAT2 but is independent of alpha/beta interferon signal transduction. J. Virol. 76 (9), 4190–4198.
Philipson, L., 1961. Adenovirus assay by the fluorescent cellcounting procedure. Virology 15, 263–268.
Pietenpol, J.A., Stein, R.W., Moran, E., Yaciuk, P., Schlegel, R., Lyons, R.M., Pittelkow, M.R., Munger, K., Howley, P.M., Moses, H.L., 1990. TGF-beta 1 inhibition of c-myc transcription and growth in keratinocytes is abrogated by viral transforming proteins with pRB binding domains. Cell 61 (5), 777–785.
Punga, T., Akusjarvi, G., 2000. The adenovirus-2 E1B-55K protein interacts with a mSin3A/histone deacetylase 1 complex. FEBS Lett. 476 (3), 248–252.
Querido, E., Blanchette, P., Yan, Q., Kamura, T., Morrison, M., Boivin, D., Kaelin, W.G., Conaway, R.C., Conaway, J.W., Branton, P.E., 2001. Degradation of p53 by adenovirus E4orf6 and E1B55K proteins occurs via a novel mechanism involving a Cullin-containing complex. Genes Dev. 15 (23), 3104–3117.
Routes, J.M., Cook, J.L., 1990. Resistance of human cells to the adenovirus E3 effect on class I MHC antigen expression. Implications for antiviral immunity. J. Immunol. 144 (7), 2763–2770.
Shao, R., Hu, M.C., Zhou, B.P., Lin, S.Y., Chiao, P.J., von Lindern, R.H., Spohn, B., Hung, M.C., 1999. E1A sensitizes cells to tumor necrosis factor-induced apoptosis through inhibition of IkappaB kinases and nuclear factor kappaB activities. J. Biol. Chem. 274 (31), 21495–21498.
Somasundaram, K., El-Deiry, W.S., 1997. Inhibition of p53-mediated transactivation and cell cycle arrest by E1A through its p300/CBP-interacting region. Oncogene 14 (9), 1047–1057.
Sturn, A., Quackenbush, J., Trajanoski, Z., 2002. Genesis: cluster analysis of microarray data. Bioinformatics 18 (1), 207–208.
White, E., 2001. Regulation of the cell cycle and apoptosis by the oncogenes of adenovirus. Oncogene 20 (54), 7836–7846.
Wold, W.S., Doronin, K., Toth, K., Kuppuswamy, M., Lichtenstein, D.L., Tollefson, A.E., 1999. Immune responses to adenoviruses: viral evasion mechanisms and their implications for the clinic. Curr. Opin. Immunol. 11 (4), 380–386.
Wu, L., Rosser, D.S., Schmidt, M.C., Berk, A., 1987. A TATA box implicated in E1A transcriptional activation of a simple adenovirus 2 promoter. Nature 326 (6112), 512–515.
Yew, P.R., Liu, X., Berk, A.J., 1994. Adenovirus E1B oncoprotein tethers a transcriptional repression domain to p53. Genes Dev. 8 (2), 190–202.
Zhao, H., Granberg, F., Elfineh, L., Pettersson, U., Svensson, C., 2003. Strategic attack on host cell gene expression during adenovirus infection. J. Virol. 77 (20), 11006–11015.
Zhao, H., Granberg, F., Pettersson, U., 2007. How adenovirus strives to control cellular gene expression. Virology 363 (2), 357–375.
Zhao, H., Boije, H., Granberg, F., Pettersson, U., Svensson, C., 2009. Activation of the interferon-induced STAT pathway during an adenovirus type 12 infection. Virology 392 (2), 186–195.